AN INSTRUMENT FOR REAL-TIME MEASUREMENTS IN ELECTRIC POWER SYSTEMS

A Thesis

Submitted to the College of Graduate Studies and Research

in Partial Fulfillment of the Requirements

for the Degree of

Master of Science

in the

Department of Electrical Engineering

University of Saskatchewan

by

ANOOP KUMAR SRIVASTAVA

Saskatoon, Saskatchewan

November 1986

dedicated to my beloved

parents

UNIVERSITY OF SASKATCHEWAN

DEPARTMENT OF ELECTRICAL ENGINEERING

CERTIFICATION OF THESIS WORK

We, the undersigned, certify that Mr. A.K. Srivastava, candidate for the Degree of Master of Science in Electrical Engineering, has presented his thesis on the subject An Instrument for Real-Time Measurement in Electric Power Systems, that this thesis is acceptable in form and content, and that this student demonstrated a satisfactory knowledge of the field covered by his thesis in an oral examination held on December 18, 1986.

External Examiner: (G.J. Sofko)
of Dept. of Physics

Internal Examiners:

December 18, 1986

COPYRIGHT

ACKNOWLEDGEMENTS

The author wishes to express his sincere thanks to Dr. H. C. Wood and Dr. M. S. Sachdev, his supervisors. With a wise and nice mix of direction and latitude, they have guided the entire course of this research.

The author takes this opportunity to acknowledge the encouragement and moral support provided by his parents and all other family members. The author is indebted to his friends, Mukesh, Atul and Lalit for their valuable suggestions and help.

The author is grateful to the University of Saskatchewan and the Natural Sciences and Engineering Research Council of Canada for providing financial assistance in the form of a scholarship.

UNIVERSITY OF SASKATCHEWAN

Electrical Engineering Abstract No. 86A279

AN INSTRUMENT FOR REAL-TIME MEASUREMENTS IN ELECTRIC POWER SYSTEMS

Student: Anoop Kumar Srivastava

Supervisors: Dr. H. C. Wood

Dr. M. S. Sachdev

M. Sc. Thesis Presented to the

College of Graduate Studies and Research

November 1986

ABSTRACT

Conventional methods of measuring electrical parameters of a power system are based on electromechanical instruments. These electromechanical instruments suffer from inherent limitations common to all mechanical systems. In recent years, digital electronic techniques have been adapted to work with electromechanical instruments, resulting in hybrid devices with better features and a clearer presentation. However, these devices also have the same limitations as the mechanical systems.

With modern developments in integrated circuit technology, microcomputers have become more powerful, yet less expensive, smaller and easier to use. This thesis presents a digital approach to measuring the operating parameters of a power system. Voltage and current signals derived from the individual phases are converted to discrete values and the system parameters are computed using a digital signal processing technique. The voltages, currents, active and reactive powers, energies, power factors, and frequency in a three phase power system are displayed, in real-time, on a standard video screen.

TABLE OF CONTENTS

LIST OF FIGURES

LIST OF TABLES

CHAPTER 1
INTRODUCTION

1.1 Background

The progress of the electrical industry to its present size and complexity in about a century is closely linked with the establishment of the science of measurement. During the 19th century the principles of electrical phenomena were discovered and applied in the development of the electrical industry. The instrumentation used during that time measured current, voltage, or resistance. The earliest measurement of current and voltage followed the Danish physicist Hans Christian Orsted's discovery in 1820 that a current-carrying wire would cause deflection in a nearby pivoted magnet [2]. A number of instruments called galvanometers were developed using that principle. These instruments used the electromagnetic force of a current to move a pointer across a scale. Either the force of gravity or the tension of a spring controlled the deflection to be proportional to the voltage across an element or the current in a circuit.

Some of the major contributors to the development of electrical measurements were Franklin, Coulomb, Volta, Ampere, Oersted, Faraday, Poggendrof, Wheatstone, and Kelvin [1]. Perhaps the most important contribution to precision direct current measurements was made by Poggendrof, who invented the potentiometer [1] which even today is used in standard laboratories for precision measurements. One of the principal influences, which led to the development of practical measuring instruments, came from the rapidly developing electrical supply industry. The electrical industry had its beginnings in the 1850s. The first few distribution systems were based on direct current. The first practical alternating current distribution system was demonstrated in 1886. With the development of the electrical industry it became necessary to quantify and measure electrical energy in order to set and control tariffs. This led to the development of wattmeters and watt-hour meters.

As instruments, which had primarily been developed at the instigation of the electricity supply industry, became more readily available they were increasingly applied

to the problems of new industries such as telephony, telegraphy and illumination which were also making great strides.

1.2 Developments in Power System Measurements

Conventional methods of measuring the electrical parameters of a power system are based on analog instruments. These instruments use principles such as the moving coil, the dynamometer, electrostatic effects, or thermal effects [3]. The majority of these instruments use electromagnetic principles and operate due to the interaction of current in a coil and a magnetic field. These techniques have been adapted and improved for several decades and continue to dominate the market. The designs of these instruments have been perfected to such an extent that only small improvements are possible, especially on commercial units. These instruments suffer from inherent errors due to mechanical moving parts and physical design constraints. The errors due to temperature changes, ageing and fatigue cannot be eliminated completely.

Research efforts over the last two decades have been directed towards the development of static instruments based on hard-wired-logic circuits. Static instruments do not have any (mechanical) moving part(s) and are based on electronic components. Those electronic circuits in which the logic design has been done using non-programmable electronic components are referred to as hard-wired-logic circuits. A number of commercial instruments are based on hard-wired-logic circuits, however, this approach has not been accepted universally for replacing conventional electromechanical instruments.

In recent years, digital electronic techniques have been adapted to work with analog instruments, resulting in hybrid devices with better features and clearer presentation of data. However, hybrid devices have the same limitations of accuracy and cost that the traditional electromechanical analog instruments have. Alternatively, modern developments in integrated circuit technology have made microcomputers more powerful, yet inexpensive, smaller, and easier to use. Consequently, the use of a microprocessor as an integral part of an instrument has become a feasible design

approach. The microprocessor, together with analog to digital converters, has made it possible to replace traditional analog instruments, static hard-wired instruments, and hybrid instruments with programmable solid state circuits.

1.3 Project Objectives

The objectives of this project were to design, construct, and test, in prototype form, a microprocessor-based digital measuring instrument for use on 3-phase power circuits. This instrument should be able to measure and display, in real time, various parameters of a power system namely, voltages, currents, active and reactive powers, energies, power factors and frequency with accuracies comparable to existing commercial instruments.

1.4 Organization of the Thesis

The thesis is organized into eight chapters and six appendices. The first chapter introduces the subject of this thesis i.e., measurements in power systems. It discusses the background and current trends in measuring techniques. In Chapter 2 various principles used in measuring instruments are described and the current trends in research in measuring techniques are discussed.

Digital algorithms, suitable for power system metering, are discussed in Chapter 3. The strengths and weaknesses of these algorithms are also discussed. Chapter 4 describes the software and hardware aspects of the design of a microprocessor-based instrument. The design considerations are discussed and the designs of the components of the instrument are described.

The system operation is discussed in Chapter 5. The software development and memory organization is also described in this chapter. Experimental test results are presented in Chapter 6. The tests were conducted on the prototype instrument for numerous operating conditions. Chapter 7 describes the conclusions drawn from the study and suggests improvements in the instrument and areas of further study. A list of bibliographic material is given in Chapter 8.

The architecture of the Intel's 8051/8052 microcontroller is described in Appendix A. Appendix B gives the details of the single board microcomputers, FX-31 and BCC-52. Appendix C presents a technique that estimates the peak value of a phasor from its real and imaginary components. Details of the analog low pass filter used in the instrument are described in Appendix D. Appendix E gives the details of a frequency multiplier circuit. The data sheets and circuit diagrams for the digitizer design are given in Appendix F. Appendix G shows the format in which the measured parameters are displayed.

CHAPTER 2

MEASUREMENTS IN POWER SYSTEMS

2.1 Introduction

Various parameters of a power system must be monitored to maintain an efficient and reliable supply of electrical power. As well, a power system must be closely monitored to ensure safe and secure operation of its generating plants. For this monitoring and for the metering of electrical energy, a power system relies upon adequate and accurate instrumentation. In this chapter various techniques for measuring electrical parameters of a power system are discussed.

2.2 General

Instruments and meters in any power system are generally provided for two main purposes. For day to day, and minute to minute running of the system and plant, operational instruments are required for example, the instruments required for generator control and for monitoring transformers and transmission and distribution systems. The metering instruments are especially required for bulk supply tariff purposes, economic assessments and plant system performance analysis for example, instruments associated with generator and power station outputs.

Some of the electrical parameters which are commonly measured and monitored in an electrical power system are listed below,

Voltage, Current, Power (active & reactive), Power Factor,
Energy (kWh & kVArh), and Frequency.

The instruments employed for measuring and monitoring the parameters of a power system are generally classified as indicating instruments, graphic instruments and data loggers. An indicating instrument displays the value of a parameter by means of the deflection of a pointer over a scale or in a digital format. Graphic instruments give a continuous record of the the power system parameters on a paper chart. A data logger

records digital data either on a magnetic tape in coded form or on a chart in numerals. The samples of one or more electrical quantities, that have been measured, are recorded at predetermined intervals of time.

2.3 Principles of Electrical Instrument Design

The principles involved in the measurement of the power system parameters are discussed in this section. The various effects of an electrical quantity which can be utilized for the operation of electrical measuring instruments are listed in Table 2.1 [3].

Table 2.1 : Electrical Instruments For Various Purposes.

Effect	Instruments
Electrolytic	Electrolytic mercury integration meter
Thermal	Hot wire ammeter, thermal demand indicator
Electrostatic	Voltmeters (wattmeters, ammeters indirectly)
Electromagnetic - Induction	ac ammeters, voltmeters, wattmeters, integration meters
Electrodynamic	Frequency meters, ac & dc wattmeters, ammeters and voltmeters

With the possible exception of the electrolytic meter, instruments embodying the effects listed in Table 1 are, in general, used for electrical measurements. The majority of instruments used for general purpose, however, fall into the category of electromagnetic,

induction or electrodynamic instruments. Some specific instruments designed using these principles are discussed in the following sections.

2.3.1 Moving-Coil Instruments

For dc measurements the permanent magnet moving coil instruments are pre-eminent. With careful design they can be made to have high accuracies making them suitable for precision measurements.

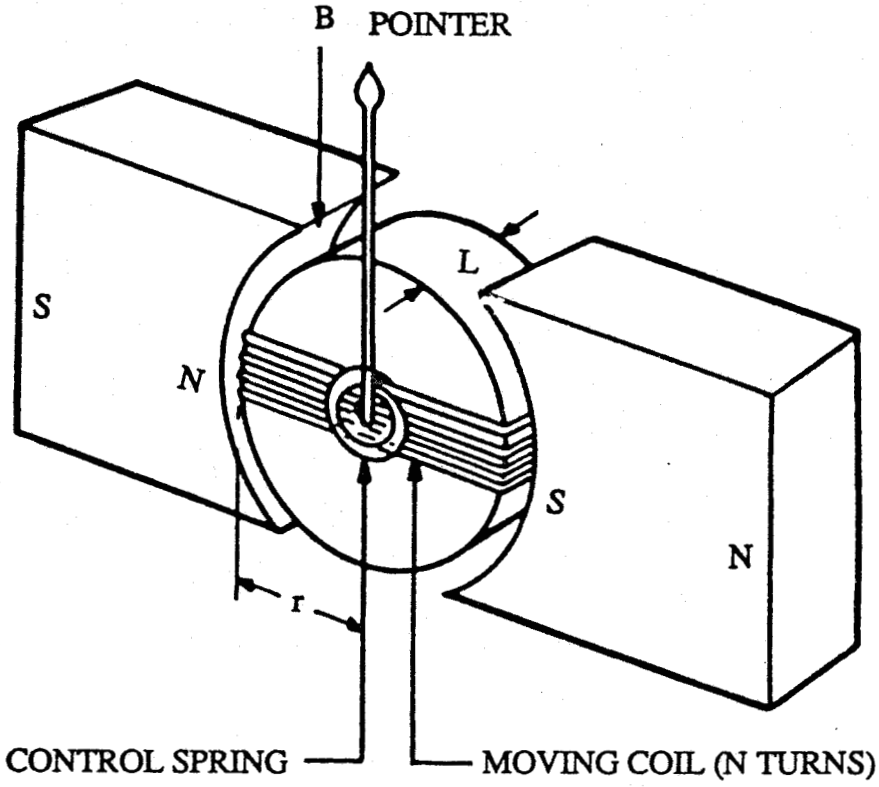

Figure 2.1. Moving-coil Instrument.

A moving coil instrument essentially consists of a pivoted coil in a radial magnetic field produced by a permanent magnet as shown in Figure 2.1 [3]. If N is the number of turns in the coil, B is the flux density in the air gap, I is the current flowing in the coil, L is the length of coil and r is the radius of the coil, then the torque, T, experienced by the moving coil can be expressed as:

$$T = NBIL \times 2r \tag{2.1}$$

To obtain a steady deflection for a constant input, the torque is balanced with the opposing torque of a coil spring. A linear characteristic is obtained by ensuring that the magnetic gap through which the moving coil passes, is made uniform. With care the angular deflection of the pointer can be made proportional to the quantity being measured. For ac measurements, the same basic design can be used with the addition of a rectifier.

2.3.2 Moving-Iron Instruments

There are two types of moving-iron instruments in common use. These are the attraction type, shown in Figure 2.2, and the repulsion type, shown in Figure 2.3 [3].

In the attraction type, the moving iron vane is drawn into the core of the coil carrying the current to be measured. The strength of the field induced in the iron vane is proportional to the current. This induced field reacts with the field due to the coil, which is also proportional to the current. The vane will thus be attracted in proportion to the square of the current.

The repulsion type consists of two soft iron pole pieces, one fixed and the other free to move. Both the iron pole pieces are situated in the coil carrying the current to be measured. The iron pole pieces are similarly magnetized and repel one another. The force between the magnetic poles, for any position, depends on the product of the pole strengths. And the pole strength of each pole depends upon the magnetic field strength which in turn is dependent upon the coil current. The instantaneous torque thus depends on the square of the instantaneous current. For both the attraction and repulsion type the magnetic effect is the same for either direction of the current.

The feature, that the torque is proportional to the square of the current, is useful in the measurement of ac quantities. The rms value of an ac quantity is the square root of the mean of the squares of the instantaneous values. Therefore, the deflection in a moving iron instrument can be made to indicate the rms value for an ac quantity, as the torque is

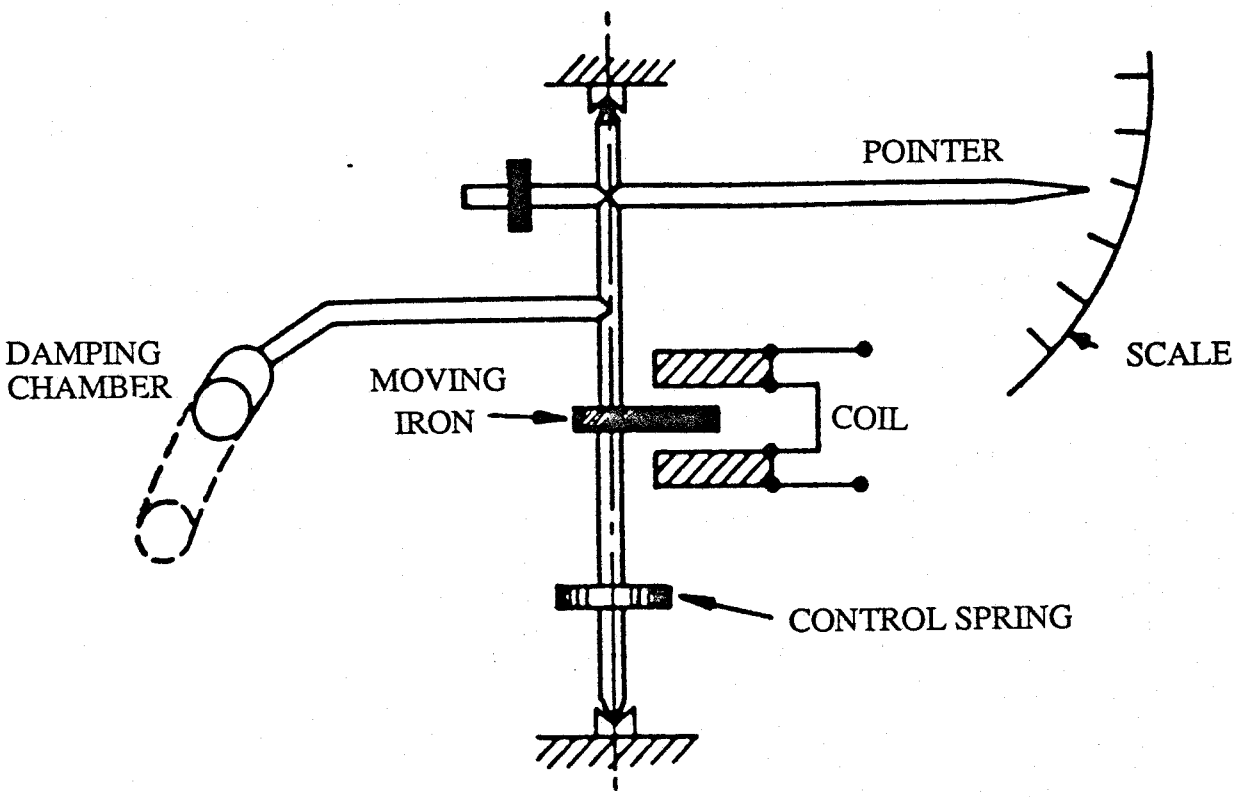

Figure 2.2. Attraction-Type Moving-Iron Instrument.

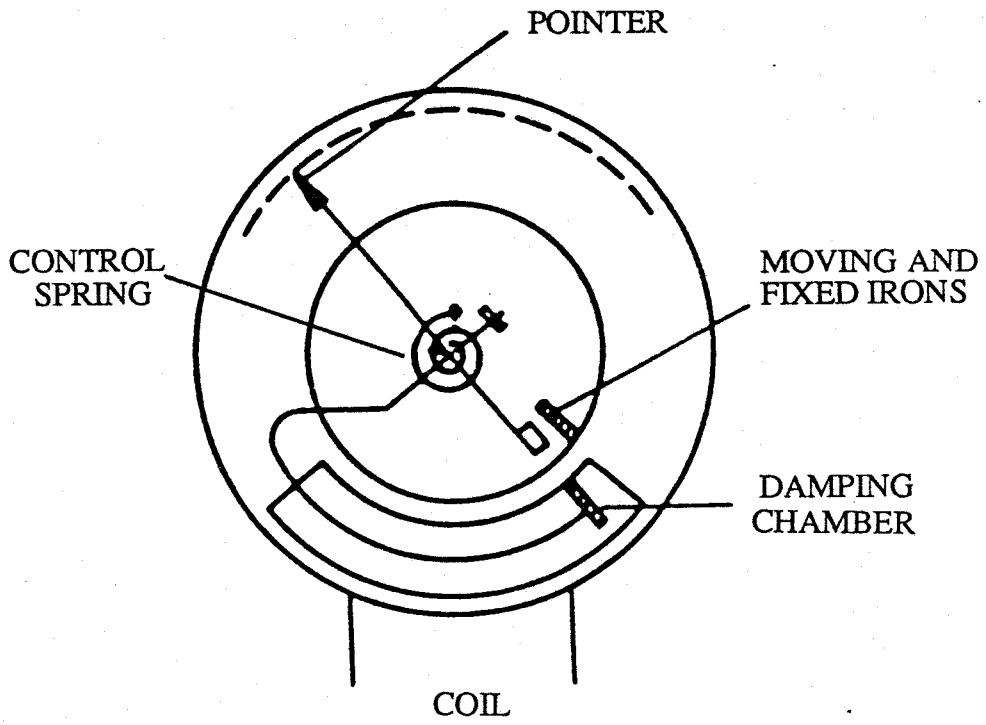

Figure 2.3. Repulsion-Type Moving-Iron Instrument.

proportional to the square of the instantaneous values of the current.

2.3.3 Dynamometer Type Instruments

The dynamometer principle can be used for the measurement of current, voltage or power, and it can be used for dc as well as ac measurements. A dynamometer type instrument consists of a moving coil which is free to move inside two fixed coils, as shown in Figure 2.4. A pointer, attached to the moving coil, indicates the value of the quantity to be measured on a scale.

For measuring current, the fixed coils carry the main current, and the moving coil is connected in parallel with the fixed coils. The coils are air-cored, thus avoiding problems of hysteresis and eddy current losses when making ac measurements. For voltage measurements the fixed and moving coils and a non inductive high resistance are connected in series.

The torque developed in the instrument is proportional to the magnetic fields due to the current in the fixed and moving coils. In the case of an ammeter, the torque is proportional to I^2 and in the case of a voltmeter, the torque is proportional to V^2 since the currents in the coils are proportional to V.

When the dynamometer principle is used for measuring power, the moving coil, in series with a high resistance, is connected to the supply voltage, V, and the current coils are connected in series with the load thus carrying the load current, I, as shown in Figure 2.5. The torque on the moving coil will thus be proportional to the product of the currents in the fixed and moving coils. Since the current in the moving system is proportional to the instantaneous voltage, the torque will be proportional to the instantaneous product of voltage and current, and therefore proportional to the active power.

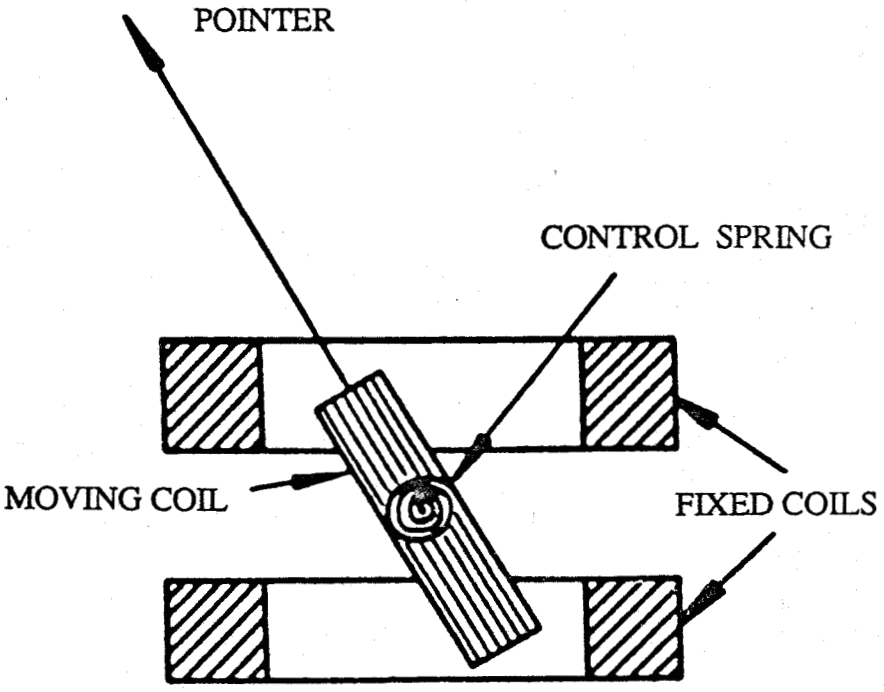

Figure 2.4. Dynamometer Coil System.

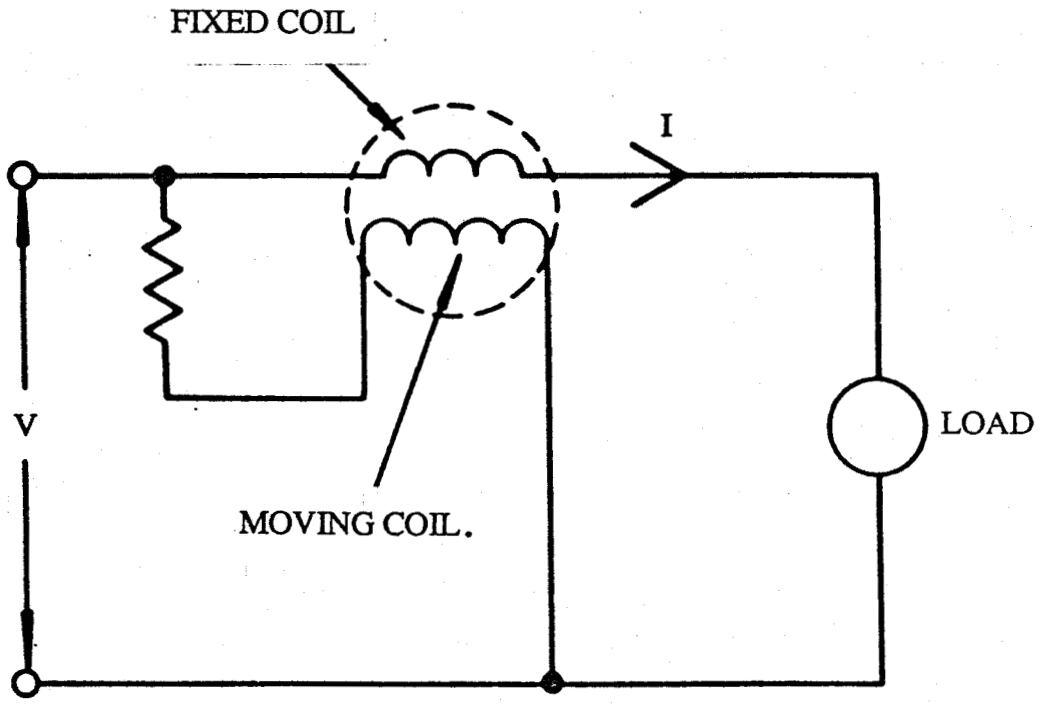

Figure 2.5 Dynamometer Wattmeter Connections.

2.3.4 Induction Ammeter and Voltmeter

This instrument operates on the same principle as the induction motor. A rotating field is produced by two pairs of electromagnets, as shown in Figure 2.6. Both pairs of electromagnets are excited from the same source. But the currents flowing in them are phase displaced by approximately 90°. This is achieved by connecting an inductance in series with one pair and a high resistance in series with the other pair. The rotating field produced by the electromagnets induces current in a non-magnetic drum or cup and causes this drum to follow the rotation of the field.

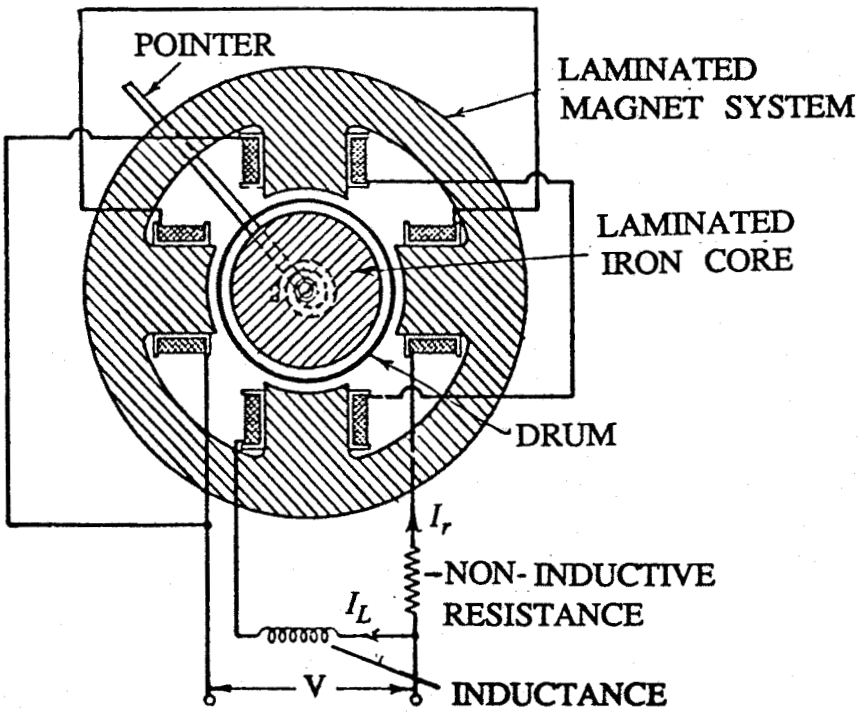

Figure 2.6. Induction type Instrument.

The current in the drum is proportional to the rotating magnetic field which is proportional to the product of the currents in the electromagnets. Thus the torque will be proportional to the square of the current (or voltage) to be measured. A spring is attached to the aluminium drum to provide the restraining torque.

2.3.5 Induction Wattmeter

The induction wattmeter has two laminated electromagnets as shown in Figure 2.7. One magnet is excited by the load current and the other magnet is excited by a current proportional to the voltage of the circuit in which the power is to be measured. A thin aluminium disc is so mounted that it is cut by the flux from both of the magnets. A deflecting torque is produced by the interaction between these fluxes and the eddy currents they induce in the disk. The voltage coil is made highly inductive, so that the resultant flux lags the voltage by about 90°. The current coil is almost non-inductive and produces a flux in phase with the current.

Figure 2.8 is an elementary vector diagram showing the relationship between the main current I, the applied voltage V, the fluxes, ϕ_i and ϕ_v due to current and voltage coils respectively, and the phase displacement ϕ between the current and the voltage. The flux ϕ_i is assumed to be in phase with the load current. The flux ϕ_v is assumed to lag behind the voltage by exactly 90 °.

If e_v & i_v and e_i & i_i are respectively the eddy e.m.f.s and currents induced in the disc due to ϕ_v & ϕ_i respectively, then it can be shown that the instantaneous torque acting on the disc is proportional to $(\phi_v i_i - \phi_i i_v)$. Furthermore, it can also be shown that the mean value of the torque is proportional to $VI\cos\phi$, [4].

2.4 Sources of Errors in Electromechanical Instruments

The electromechanical instruments indicating the electrical parameters, such as voltage and current by the use of a mechanical needle pointing over a dial have their limitations. Effects such as friction and temperature cause errors in all electromechanical instruments. If the errors are to be kept to a minimum, the mass of the moving system must be kept small and the bearings should have as little friction as possible. The best results are obtained when the ratio of the torque to the mass of the moving system is large.

In the moving coil instruments, a major source of error is the changes in resistance of the instrument windings due to temperature changes. Much effort in instrument design

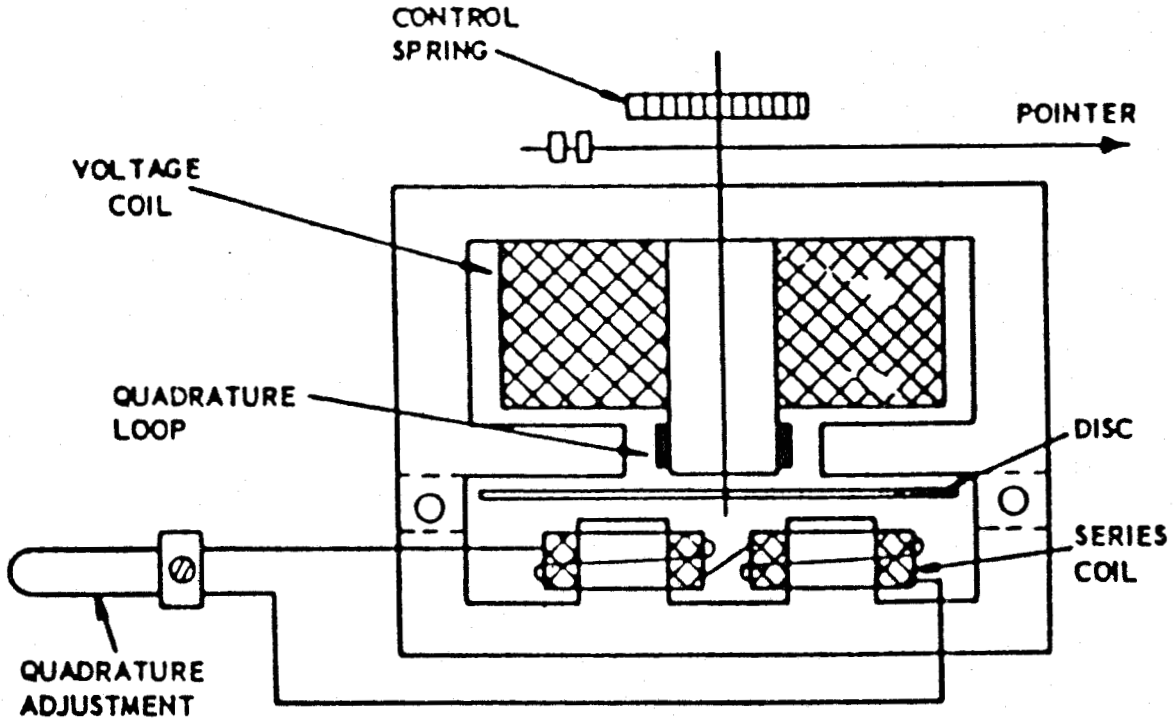

Figure 2.7. Induction Wattmeter.

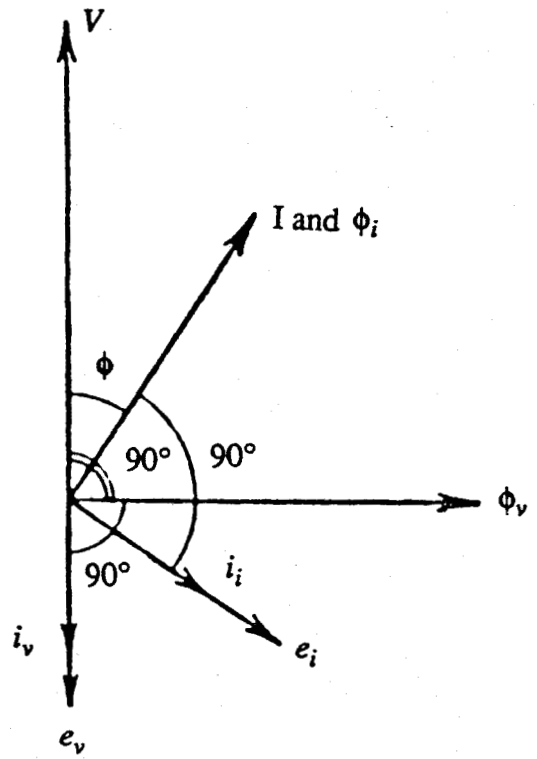

Figure 2.8. Vector Relationship in Induction Wattmeter.

is directed to compensate for resistance changes.

In the moving iron instruments, the main source of error is the hysteresis of the magnetic circuit. This error is usually minimized by using a nickel-iron alloy for the core. Changes in the system frequency change the impedance of the voltage coil producing errors in an ac voltmeter.

Frictional errors can occur in dynamometer type instruments due to the comparatively low torque and large mass of the moving coils. In this case the torque to mass ratio is small. Temperature errors can also occur in the same way as in the moving coil instruments.

The errors in the induction instruments are mainly due to the variations in the frequency, causing changes in the impedance of the winding, and the temperature. Other mechanical elements such as springs can also be a source of error in electromechanical instruments.

2.5 Current Trends in Metering

With the advent of semiconductor technology there has been a considerable amount of research in the field of hard-wired and programmable instrumentation. A number of instruments which are based on hard-wired logic are available commercially. These instruments have not been universally accepted for the replacement of the devices which are based on electromechanical principles.

Recently, considerable research has been conducted in the field of digital instruments based on microprocessors. With the developments in the integrated circuit technology, the components have become cheaper, smaller and easier to use. Therefore, the use of microprocessors as integral parts of instrumentation and control in power systems is an attractive alternative to hard-wired logic or electromechanical devices.

One of the major advantages of using the microprocessor based instruments is that they are software based systems and, therefore, can be adapted readily for different circumstances. That is, with the same hardware, different functions can be performed simply by changing the software. The system, therefore, is much more flexible and could

lead to reduction in cost.

Another advantage of using the programmable instruments is that the measured parameter is available in the digital format. Since many electric sub-stations use computers for control and data logging applications, the digital output of the instruments can be directly presented to the computer.

Other advantages of digital systems are that the data displayed is in the digital format and, therefore, can be read more easily [5]. The digital devices have higher input impedances and, therefore, present lesser burdens to the transducers. Also, the levels of the input signal required are much lower compared to those required for the electromechanical instruments.

2.6 Concluding Remarks

In this chapter various techniques for measurement of power system parameters are discussed. Some of the basic principles used in electromechanical instruments are also presented. The current trends in power system instrumentation are highlighted. Some advantages of using digital instruments over the conventional electromechanical types are also discussed. In digital instruments the measurements are performed by a few mathematical manipulations on the values of the samples of the input signal. These mathematical manipulations are called algorithms. Some of the algorithms suitable for the metering applications in power systems are described in the next chapter.

CHAPTER 3

ALGORITHMS FOR POWER SYSTEM METERING

3.1 Introduction

There are a number of well established algorithms for estimating the operating parameters of a power system from sampled values of voltages and currents. These algorithms usually consist of a few mathematical equations that are implemented to produce numerical estimates of frequency and components of voltage and current phasors. Derived quantities such as power and energy can also be determined. These algorithms have been developed over the last fifteen years as a result of substantial research [10,18] into the techniques for estimating the peak value and phase angle of voltage and current phasors.

This chapter reviews the mathematical basis of the algorithms that can compute the magnitudes and phase angles of phasors representing voltage and current waveforms.

3.2 Algorithms

The algorithms proposed in the literature can be classified into categories of trigonometric, correlation, and least error squares approach. This classification is based on the mathematical techniques used in developing the algorithms. The discussion in this section assumes that signals being processed are power system voltages. Similar procedures can be used for processing data representing power system currents.

3.2.1 Trigonometric Algorithms

The trigonometric algorithms assume that the waveforms of voltages and currents are sinusoids of the fundamental frequency. Some harmonics and noise arise in power systems because of non-linearities in the system and loads. Analog filters can be used to eliminate the noise and non-fundamental frequency components. For a sinusoidal voltage of the fundamental frequency, the instantaneous voltage can be expressed as follows:

$$v = V_p \sin(\omega_0 t + \theta_v) \tag{3.1}$$

where

v is the instantaneous value of the voltage,

V_p is the peak value of the voltage,

ω_0 is the nominal frequency,

t is the time in seconds,

and θ_v is the phase angle at $t = 0$.

The trigonometric algorithms are based on this equation and its derivatives. The first and the second derivatives of the voltage can be expressed by Equations 3.2 and 3.3, respectively:

$$\dot{v} = \omega_0 V_p \cos(\omega_0 t + \theta_v) \tag{3.2}$$

and

$$\ddot{v} = -\omega_0^2 V_p \sin(\omega_0 t + \theta_v). \tag{3.3}$$

Three different trigonometric algorithms are described in this section. These are the Makino and Miki algorithm [6], the Mann and Morrison algorithm [7], and the Gilcrest, Rockfeller and Udren algorithm [8,9].

3.2.1.1 Makino and Miki Algorithm

Makino and Miki [6] proposed an algorithm that requires two samples of the signal that is to be processed. Using Equation 3.1 the instantaneous values of a voltage waveform at times $(k-1)\Delta T$ and $k\Delta T$ can be represented as:

$$v_{k-1} = V_p \sin(\omega_0 t + \theta_v - \omega_0 \Delta T) \tag{3.4}$$

and

$$v_k = V_p \sin(\omega_0 t + \theta_v). \tag{3.5}$$

Using the well known rules of trigonometry, Equation 3.4 can be expanded to the following form:

$$v_{k-1} = V_p \sin(\omega_0 t + \theta_v) \cos(\omega_0 \Delta T) - V_p \cos(\omega_0 t + \theta_v) \sin(\omega_0 \Delta T). \tag{3.6}$$

Substituting in this equation the value of $V_p \sin(\omega_0 t + \theta_v)$ from Equation 3.5, and rearranging, Equation 3.7 can be obtained as follows:

$$V_p \cos(\omega_0 t + \theta_v) = \frac{v_k \cos(\omega_0 \Delta T) - v_{k-1}}{\sin(\omega_0 \Delta T)}. \tag{3.7}$$

The peak value of the phasor representing the voltage waveform can now be estimated by squaring and adding Equations 3.5 and 3.7 as follows:

$$V_p = \left\{ v_k^2 + \left[\frac{v_k \cos(\omega_0 \Delta T) - v_{k-1}}{\sin(\omega_0 \Delta T)} \right]^2 \right\}^{\frac{1}{2}}. \tag{3.8}$$

The phase angle can similarly be determined from Equations 3.5 and 3.7 as follows:

$$\omega_0 t + \theta_v = \arctan \frac{v_k \sin(\omega_0 \Delta T)}{v_k \cos(\omega_0 \Delta T) - v_{k-1}}. \tag{3.9}$$

3.2.1.2 Mann and Morrison Algorithm

Mann and Morrison [7] used the values of the samples and the first derivatives to estimate the peak values and phase angles of the phasors representing the input sinusoidal voltage and current waveforms. They also suggested that the first derivative, $\dot{v}$, can be estimated from three consecutive samples of the voltage. If three samples of a voltage are taken at $(k-1)\Delta T$, $k\Delta T$ and $(k+1)\Delta T$ seconds, the first derivative at time $k\Delta T$ can be estimated as follows:

$$\dot{v} = \frac{(v_{k+1} - v_{k-1})}{2\Delta T}. \tag{3.10}$$

Substituting for $\dot{v}$ from Equation 3.2 it follows that

$$V_p \cos(\omega_0 t + \theta_v) = \frac{v_{k+1} - v_{k-1}}{2\omega_0 \Delta T}. \tag{3.11}$$

Using these expressions the peak value and phase angle of the phasor representing the voltage waveform can be estimated from Equations 3.5 and 3.11 as follows:

$$V_p = \left\{ v_k^2 + \left[\frac{v_{k+1} - v_{k-1}}{2\omega_0 \Delta T} \right]^2 \right\}^{\frac{1}{2}} \tag{3.12}$$

$$\omega_0 t + \theta_v = \arctan \frac{2v_k \omega_0 \Delta T}{v_{k+1} - v_{k-1}}. \tag{3.13}$$

3.2.1.3 Gilcrest, Rockfeller and Udren Algorithm

Gilcrest et al. [8,9] used the first and second derivatives of voltages and currents to estimate the peak values and phase angles of the phasors representing them. This approach was used to minimize the effect of the dc offsets that are present in voltages and currents. The proposed technique uses three samples of a sinusoidal voltage taken at times $(k-1)\Delta T$, $k\Delta T$ and $(k+1)\Delta T$. The first derivatives of the voltage at times $(k-\frac{1}{2})\Delta T$ and $(k+\frac{1}{2})\Delta T$ can be approximated as follows:

$$\dot{v}_{-\frac{1}{2}} = \frac{v_k - v_{k-1}}{\Delta T} \tag{3.14}$$

and

$$\dot{v}_{+\frac{1}{2}} = \frac{v_{k+1} - v_k}{\Delta T}. \tag{3.15}$$

The first derivates obtained from Equations 3.14 and 3.15 can now be used to estimate the second derivative at time $k\Delta T$ using the following equations:

$$\ddot{v}_k = \frac{1}{\Delta T}\left\{ \dot{v}_{+\frac{1}{2}} - \dot{v}_{-\frac{1}{2}} \right\} \tag{3.16}$$

and

$$\ddot{v}_k = \left(\frac{1}{\Delta T}\right)^2 (v_{k+1} - 2v_k + v_{k-1}). \tag{3.17}$$

Substituting for $\ddot{v}$ from Equation 3.3 it follows that

$$V_p \sin(\omega_0 t + \theta_v) = -\left(\frac{1}{\omega_0 \Delta T}\right)^2 (v_{k+1} - 2v_k + v_{k-1}). \tag{3.18}$$

Using this technique the peak value and phase angle of the phasors representing the voltage waveform can be estimated from Equations 3.18 and 3.11 as follows:

$$V_p = \left(\frac{1}{\omega_0 \Delta T}\right)\left\{\left[\frac{v_{k+1} - v_{k-1}}{2}\right]^2 + \left[\frac{v_{k+1} - 2v_k + v_{k-1}}{\omega_0 \Delta T}\right]^2\right\}^{\frac{1}{2}} \tag{3.19}$$

$$\omega_0 t + \theta_v = \arctan - \frac{2(v_{k+1} - 2v_k + v_{k-1})}{\omega_0 \Delta T (v_{k+1} - v_{k-1})}. \tag{3.20}$$

3.2.1.4 Strengths and Weaknesses

Since the trigonometric algorithms discussed above use short data windows, they respond rapidly to the changes in the data and also require only a few computations for their implementation. But, on the other hand, they amplify noise that might be present in the input data. Also, the accuracy of the computed values of phasors is adversely affected by the presence of decaying dc and high frequency components in system voltages and currents [10].

3.2.2 Correlation Algorithms

The process of correlating an input waveform with a set of orthogonal functions can be used to extract components of selected frequencies from the input waveform. Several orthogonal functions have been proposed in the past for use in digital relaying applications. The most common orthogonal function pairs used in power system

applications are sine and cosine functions, and even and odd rectangular waves.

Ramamoorty [11] suggested that the information concerning the voltage and current phasors at fundamental frequency can be extracted by correlating the data samples of one cycle with the samples of sine and cosine waves at that frequency. The correlation of a signal with unit amplitude sine and cosine waveforms can be used to extract the real and imaginary components of a phasor. This process can be expressed mathematically as follows:

$$v_r = \frac{1}{\pi} V_p \int_0^{2\pi} \sin(\omega_0 t + \theta_v) \sin(\omega_0 t)\, d(\omega_0 t) \tag{3.21}$$

and

$$v_i = \frac{1}{\pi} V_p \int_0^{2\pi} \sin(\omega_0 t + \theta_v) \cos(\omega_0 t)\, d(\omega_0 t) \tag{3.22}$$

where

V_p is the peak value of the voltage,

v_i is the imaginary part of the fundamental frequency voltage phasor, and

v_r is the real part of the fundamental frequency voltage phasor.

From the sampling process the input signals are available at discrete instants of time and the numerical techniques are used to evaluate the integrations. Using the rectangular rule of integration, the real and imaginary parts of the voltage phasor can be estimated from the following equations:

$$v_r = (\frac{2}{m}) \sum_{n=0}^{m-1} v_{k+n-m+1} \sin(\frac{2\pi n}{m}) \tag{3.23}$$

and

$$v_i = (\frac{2}{m}) \sum_{n=0}^{m-1} v_{k+n-m+1} cos(\frac{2\pi n}{m}) \tag{3.24}$$

where

v_j is the value of the voltage samples, and

m represents the number of samples taken in one cycle.

The peak value and phase angle of the voltage phasor can be determined as follows:

$$V_p = \sqrt{v_r^2 + v_i^2} \tag{3.25}$$

$$\theta_v = arctan\ (\frac{v_i}{v_r}). \tag{3.26}$$

This procedure which is essentially a Fourier analysis can be extented to use multiple cycles of data to extract the phasor quantities. Phadke et al. [12], applied this correlation approach using a data window of one half cycle plus one sample for faster response. The accuracy of results obtained by this approach is affected by the presence of non-fundamental frequency components and by the dc offsets.

Another variation to this approach consists of correlating the data with the even and odd rectangular waves [13]. These waves are shown in Figure 3.1 and can be mathematically defined as follows:

$$W_r(t) = signum \left\{ \sin(\omega_0 t) \right\} \tag{3.27}$$

and

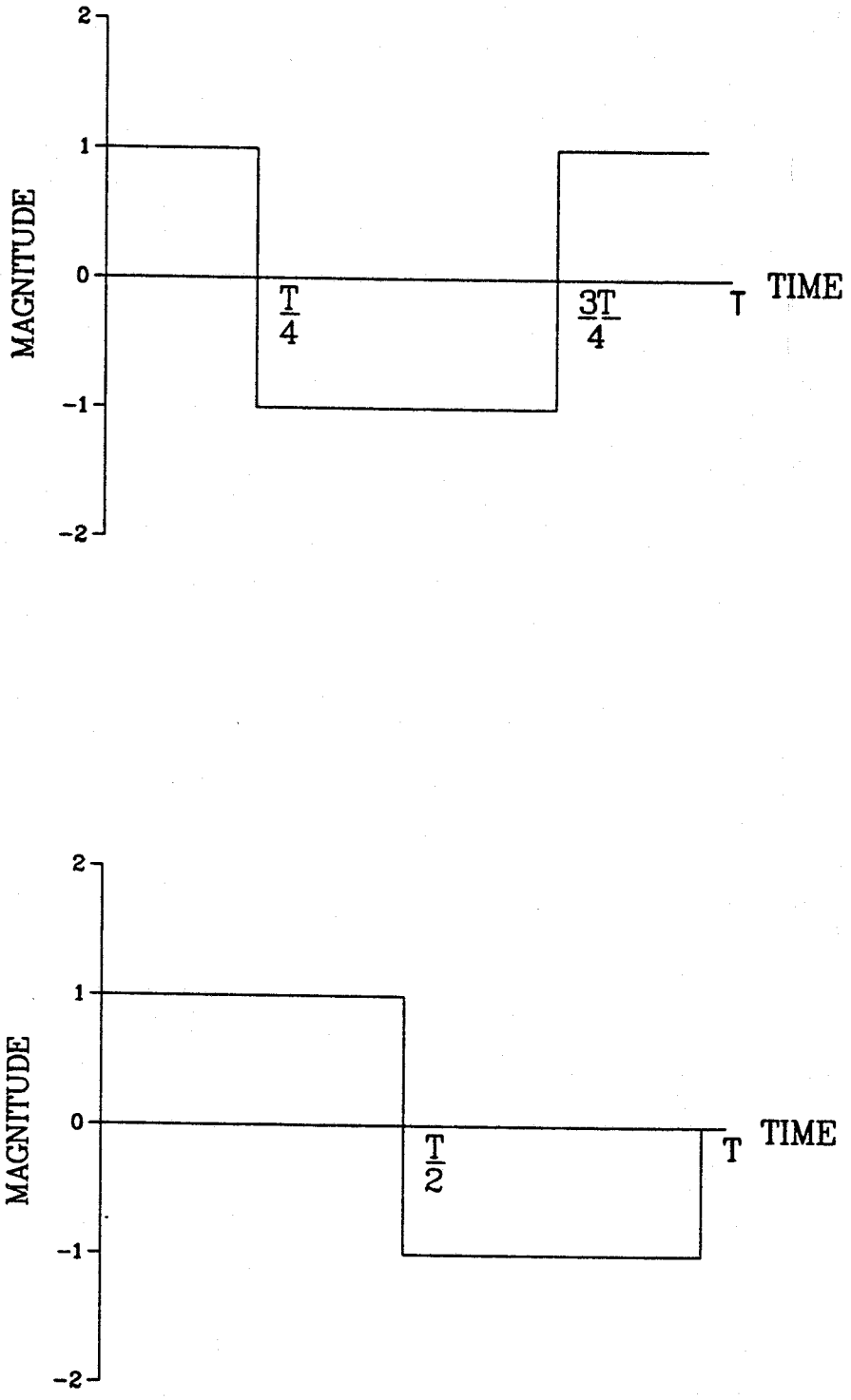

Figure 3.1. Even and Odd rectangular waves.

$$W_i(t) = signum\left\{\cos(\omega_0 t)\right\} \tag{3.28}$$

where

$$signum\ (x) = \begin{cases} 1 & \text{if } x > 0 \\ 0 & \text{if } x = 0 \\ -1 & \text{if } x < 0 \end{cases},$$

$W_r(t)$ is the odd rectangular wave, and

$W_i(t)$ is the even rectangular wave.

The real and imaginary components of the fundamental frequency voltage phasor can be determined using Equations 3.29 and 3.30.

$$v_r = (\frac{1}{A}) \sum_{n=0}^{m-1} v_{k+n-m+1}\ signum\left\{ sin(\frac{2\pi n}{m}) \right\} \tag{3.29}$$

$$v_i = (\frac{1}{A}) \sum_{n=0}^{m-1} v_{k+n-m+1}\ signum\left\{ cos(\frac{2\pi n}{m}) \right\} \tag{3.30}$$

where

A is a scaling factor,

v_k is the latest sample of the input signal, and

m is the total number of samples in the data window.

An advantage of correlating with the even and odd rectangular waves is that the computations consist of additions and subtractions only. Further details of this technique

are given in the following chapter.

3.2.2.1 Strengths and Weaknesses

The Fourier analysis and Even-Odd rectangular wave algorithms use large data windows (16 ms or larger). Therefore, their transient response is slower than that of the short window algorithms and the implementation time is greater. These algorithms do however attenuate noise and reject high frequency components quite effectively. Even the non-decaying dc components of the dc offsets in the voltages and currents are rejected. The accuracy of the results is affected only by the decaying component of the dc offsets which occurs when the system is in a transient state [10].

3.2.3 Least Error Squares Approach

Luckett et al. [14], proposed the use of the least error squares approach for computing the peak values and phase angles of voltage and current phasors. Brooks [15], also used the least error squares approach in which he assumed that the input signal is composed of a dc component and a fundamental frequency component. Sachdev and Baribeau [16], reported further developments in this approach and demonstrated that a major part of the computations required for the algorithm can be performed off-line. The procedure to implement the least error squares technique can be briefly described as selecting a suitable model for the signal and linearizing the model. After linearizing the model, the equations are expressed in the matrix form and the values of the elements of the matrix are estimated.

For a sinusoidal voltage waveform at the fundamental frequency the instantaneous voltage can be expressed as follows:

$$v(t) = V_p \sin(\omega_0 t + \theta_v) \tag{3.31}$$

where

$v(t)$ is the instantaneous value of the voltage,

V_p is the peak value of the voltage,

ω_0 is the nominal frequency,

t is the time in seconds,

and θ_v is the phase angle at $t = 0$.

By expanding the $sin(\omega_0 t + \theta_v)$ term in Equation 3.31 the following equation can be obtained:

$$v(t) = V_p \cos\theta_v \; sin(\omega_0 t) + V_p \sin\theta_v \; cos(\omega_0 t). \tag{3.32}$$

At any instant of time $t=t_1$, this equation can be written as follows:

$$v(t_1) = V_p \cos\theta_v \; sin(\omega_0 t_1) + V_p \sin\theta_v \; cos(\omega_0 t_1). \tag{3.33}$$

Since $\omega_0 t_1$ is a constant for this instant of time, this equation can be written in the following linear form:

$$v(t_1) = a_{11} x_1 + a_{12} x_2 \tag{3.34}$$

where

$$x_1 = V_p \cos\theta_v, \qquad a_{11} = sin(\omega_0 t_1),$$

$$x_2 = V_p \sin\theta_v, \qquad a_{12} = cos(\omega_0 t_1).$$

Assuming that the voltage is sampled at intervals of ΔT seconds, the next sample received at time $t_2 = (t_1 + \Delta T)$ can be described as follows:

$$v(t_1+\Delta T) = a_{21}x_1 + a_{22}x_2. \tag{3.35}$$

For a preselected time reference and a preselected sampling rate, the values of the a coefficients are known for a particular frequency. If p samples are taken, the equations can be written in the following matrix form:

$$\underset{p\times 1}{\left[v \right]} = \underset{p\times 2}{\left[A \right]} \underset{2\times 1}{\left[X \right]}. \tag{3.36}$$

For p greater than two, the vector of unknowns, $\left[X \right]$, can be determined by using the following equation,

$$\underset{2\times 1}{\left[X \right]} = \underset{2\times p}{\left[A \right]^{\dagger}} \underset{p\times 1}{\left[v \right]}. \tag{3.37}$$

In this equation, $\left[A \right]^{\dagger}$ is the left pseudo inverse of $\left[A \right]$ and is defined as

$$\underset{2\times p}{\left[A \right]^{\dagger}} = \underset{2\times p}{\left[\underset{p\times 2}{\left[A \right]^{T}} \underset{p\times 2}{\left[A \right]} \right]^{-1}} \underset{2\times p}{\left[A \right]^{T}}. \tag{3.38}$$

Since the elements of the matrix $\left[A \right]$ are known a priori, the elements of the left pseudoinverse matrix can be determined off-line. This substantially reduces the on-line calculations required to estimate the real and imaginary components of the phasors when the least error squares technique is used.

3.2.3.1 Strengths and Weaknesses

The Least Error Square algorithm rejects the high frequency components and decaying dc component very effectively. It also attenuates noise as the signals are processed. The transient response of this algorithm, however, is slower than the short window algorithms. The implementation time for this algorithm is large compared to the correlation algorithms as the implementation requires more multiplications [10].

3.3 Concluding Remarks

In this chapter, a number of algorithms suitable for metering in power system, have been discussed. These algorithms are the Makino and Miki, Mann and Morrison, Rockfeller and Urden, Fourier analysis, Even-Odd, and Least Error Square algorithms. It is shown that the power system signals, voltages and currents, can be manipulated by trigonometric, correlation, and least error square approximation techniques to evaluate the values of voltage and current phasors. Derived parameters such as power, energy, power factor etc., can also be computed from the values of voltage and current phasors.

Each of the algorithms discussed in this chapter has its strengths and weaknesses. In order to design a measurement system the choice of algorithm should be made by weighing their strengths and weaknesses. The selection of an appropriate algorithm and the design of the measurement system are described in the next chapter.

CHAPTER 4

DESIGN OF THE INSTRUMENT

4.1 Introduction

The objective of this project is to design, implement and test a microprocessor based instrument to monitor and display, in real time, various parameters of a power system. The parameters under consideration are Voltages, Currents, Active Powers, Reactive Powers, Power Factors, Energies (kWh & kVArh) and Frequency.

This chapter describes the design for such an instrument. The description is divided into two main sections: software and hardware.

4.2 Requirement Specifications

The first step in the project was to select the general specifications that describe, in a broad sense, the operating requirements of the instrument. The selected specifications [21] are summarized in the following list:

1. Purpose : The instrument is required to measure voltages at power system buses and currents in lines, transformers etc. and display in real time the following parameters, for each phase, in a 3-phase power system:

(a) RMS Voltage,

(b) RMS Current,

(c) Active Power and Reactive Power,

(d) Power factor,

(e) Energy (kWh & kVArh), and

(f) Frequency.

2. Input : The inputs to the instrument are to be,

(a) Phase to ground voltages of the three phases (scaled down to 2.5 volts for rated value) and

(b) Three phase currents converted to voltages (2.5 volts for rated value).

3. **Accuracy :** The accuracy of measurements has been selected as 1% class as defined in ANSI standard number C39.1 [19]. The accuracy for the switchboard type instruments is specified as 1% in IEEE standard 120-1955 [20]. From this standard the accuracy requirement for frequency is 0.05 Hz and the accuracy requirement for power factor is 0.02.

4. **Input Waveform :** The waveforms of all the inputs are to be sinusoids of the fundamental frequency. The components of all other frequencies are to be removed by filtering.

5. **Output :** The output of the instrument is a real time display, in a digital format, of the above listed parameters.

6. **User Input :** The user is required to input the rated values of the power system voltages and currents.

7. **User Interface :** A keyboard and a monitor is to provide an interface between the user and the instrument.

8. **Overload Capacity :** The levels of all inputs are to be upto 150% of the rated values without causing saturation.

9. **Operating Range of the Instrument :** The operating ranges of the instrument are to be,

Voltage	: 0 to 150% 0f the rated value,
Current	: 0 to 150% 0f the rated value,
Power (Active & Reactive)	: Display upto 6 digits,
Energy (kWh & kVArh)	: Display upto 6 digits,
Power Factor	: - 0.5 to + 0.5, and
Frequency	: 55 Hz to 65 Hz.

10. Out of Range Protection : The instrument is to be protected against the inputs beyond the operating range.

4.3 System Implementation

The selected electrical parameters can be measured in many different ways. The conventional methods of measuring electrical parameters are based on electromechanical analog instruments as discussed in chapter 2. These techniques have been adapted and improved for several decades and still dominate the market. Another method of measuring electrical parameters is by static instrumentation that is based either on hard-wired-logic or on programmable logic.

The number of parameters to be determined by the proposed instrument makes the task of measurement very complex. To perform the task, a static instrument based on programmable logic is designed. It uses the most common method of implementing programmable logic, a microcomputer. The present day microcomputers work on a clock rate of a few MHz and perform simple arithmetic and logic functions at this speed. However, for more complex operations such as multiplications and divisions, microcomputers take several clock cycles.

4.4 Software

This section describes the functions of the software that is incorporated into the prototype instrument. In general, the purpose of the software is to control the instrument and to implement the algorithms required to compute various parameters. The specific tasks for controlling the instrument are, user interaction, display of the output in a digital format and control of digitization process. The computation of voltage and current phasors from the samples of voltages and currents is implemented using the software. The calculated voltage and current phasors are then used to compute the rms values of voltage and current, the active and reactive powers, energies and power factors.

4.4.1 Algorithm Selection

Each algorithm proposed in the previous chapter has its strengths and weaknesses. Since many parameters are to be measured, the number of computations and hence the time required for the computations is expected to be large. Therefore, the selected algorithm should require very short processing time so that the computations can be repeated at short intervals of time. This affects the response time of the instrument which is an important parameter in a real time application. In a metering application accuracy is of prime importance. Therefore, the criteria of time and accuracy have been used to select an appropriate algorithm.

The computation time required by the algorithms discussed earlier depends upon the number of samples that have to be considered at any instant. It also depends on the number and type of computations required, for example, the number of additions, subtractions, multiplications or divisions to be performed during each set of the computations. Most algorithms are designed considering that the inputs are sinusoids of the fundamental frequency. Some algorithms use short data windows (two to five consecutive samples). These algorithms, therefore, require few computations which can be performed in very short time compared to one cycle of the fundamental frequency. The algorithms which can work well on distorted waveforms use long data windows (eight to sixteen consecutive samples) and, therefore, for the same type of computations, require more time.

The power system voltages and currents are sometimes distorted and contain several non-fundamental components. Long window algorithms are, therefore, expected to provide more accurate results than the short window algorithms [10]. Since, in a measuring instrument, the accuracy is of prime importance, a long window algorithm has been selected for this application.

Among the long window algorithms presented in the previous chapter, the Even and Odd Rectangular Waves (EORW) algorithm requires the least complex computations. These computations consist of additions and subtractions only because the correlation functions are even and odd rectangular waves. By contrast the Fourier algorithm

correlates the data with sine and cosine functions and, therefore, requires that data be multiplied with weighting factors. Similarly, the least error squares technique uses multiplications which require more processing time than addition for the selected technology. Also the accuracy of the EORW algorithm is comparable to the accuracy of other long window algorithms. Therefore, the EORW algorithm was selected.

4.4.1.1 The Even and Odd Rectangular Waves Algorithm

As discussed in the previous chapter the EORW algorithm is a correlation algorithm in which the signal to be evaluated is correlated with a set of orthogonal even and odd functions. These functions can be mathematically represented as:

$$W_r(t) = signum\left\{\sin(\omega_0 t)\right\} \tag{4.1}$$

$$W_i(t) = signum\left\{\cos(\omega_0 t)\right\} \tag{4.2}$$

where

$$signum\ (x) = \begin{cases} 1 & \text{if } x > 0 \\ 0 & \text{if } x = 0, \\ -1 & \text{if } x < 0 \end{cases}$$

$W_r(t)$ is the odd rectangular wave, and

$W_i(t)$ is the even rectangular wave.

The real and imaginary parts of a fundamental frequency voltage phasor can now be determined by using Equations 3.29 and 3.30.

$$v_r = (\frac{1}{A}) \sum_{n=0}^{m-1} v_{k+n-m+1}\, Signum \left\{ sin(\frac{2\pi n}{m}) \right\} \tag{4.3}$$

$$v_i = (\frac{1}{A}) \sum_{n=0}^{m-1} v_{k+n-m+1}\, Signum \left\{ cos(\frac{2\pi n}{m}) \right\} \tag{4.4}$$

where

A is a scaling factor,

v_k is the latest sample, and

m is the total number of samples in a data window.

Equations 4.1 and 4.2 show that the value of function $signum(x)$ can be either +1, 0, or -1. The computations required in Equations 4.3 and 4.4, therefore, consist of additions and subtractions only.

4.4.1.2 Frequency Response of the EORW Algorithm

The frequency response of EORW algorithm is illustrated in Figure 4.1. An expanded version of the first maximum is shown in Figure 4.2. This frequency response has been plotted for a sampling rate of 480 samples/sec. It is observed that the response near the nominal frequency is such that with a decrease in the frequency the output of the algorithm increases and with an increase in the frequency the output decreases. These changes in the frequency response could introduce errors in computations of voltage and current phasors. The accuracy of the derived parameters would also be affected.

To avoid the problem of errors due to the drift in frequency, it was decided to make the sampling rate variable so that the number of samples per cycle of the fundamental frequency remains constant. By making the number of samples per cycle constant, the sampling frequency is made a fixed multiple of the incoming signal frequency. Therefore, the gain of the algorithm remains constant for all the values of the frequency

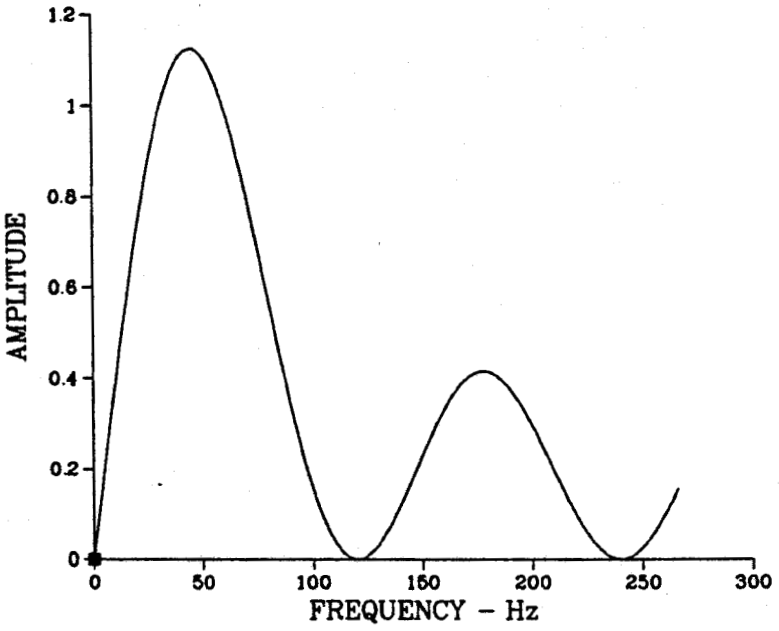

Figure 4.1. Frequency Response of Even-Odd Algorithm.

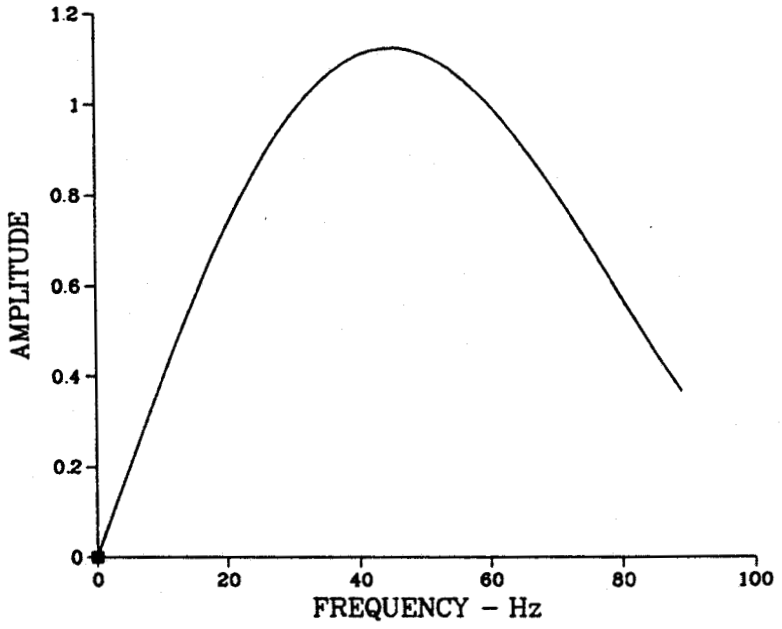

Figure 4.2. First Maximum of the Frequency Response.

of the input signal.

Another important observation from the frequency response (Figure 4.1) is that the algorithm filters out the even harmonics of the nominal frequency. This fact can be used in the design of analog filters which are necessary to remove unwanted components from the input signals. The design of the analog filters is discussed in a succeeding section.

4.4.3 Computation of the Peak/RMS Values

The peak value of a phasor can be calculated from the real and imaginary components of the phasor by using the following expression:

$$Peak\ Value = V_p = \sqrt{V_{re}^2 + V_{im}^2} \tag{4.5}$$

If this expression has to be implemented on a microcomputer, the computation time will be substantial as this expression involves two multiplications and a square root function. However, the expression can be approximated by the Piecewise Linear Approximation technique [22]. The approximations reduce the processing time but they introduce some errors in the the final results. In this application, a four region approximation is used. The mean value of the error for this approximation is 1.3972×10^{-4} [22]. The details of the linear approximation technique are discussed in Appendix C.

4.4.4 Computation of Power

For the computation of power, the real and imaginary components of the voltage and current phasors can be used. If $I_A \cos\theta_i$ and $I_A \sin\theta_i$ are respectively the real and imaginary components, I_r & I_i, of the phase-A current and $V_A \cos\theta_v$ and $V_A \sin\theta_v$ are respectively the real and imaginary components, V_r & V_i, of the voltage in the same phase, then the active power can be computed as follows:

$$Active\ Power = V_A I_A \cos(\theta_v - \theta_i) \tag{4.6}$$

$$= V_A I_A [\cos\theta_v \cos\theta_i + \sin\theta_v \sin\theta_i]$$

$$= V_A \cos\theta_v I_A \cos\theta_i + V_A \sin\theta_v I_A \sin\theta_i$$

$$= V_r I_r + V_i I_i \tag{4.7}$$

where

I_A & V_A are peak values of voltage and current respectively in phase A, and θ_v & θ_i are respectively the angle associated with the voltage and current phasors measured with respect to a common reference.

Similarly reactive power can be computed as follows:

$$Reactive\ Power = V_A I_A \sin(\theta_v - \theta_i) \tag{4.8}$$

$$= V_A I_A [sin\ \theta_v \cos\theta_i - \cos\theta_v \sin\theta_i]$$

$$= V_A \sin\theta_v I_A \cos\theta_i - V_A \cos\theta_v I_A \sin\theta_i .$$

$$= V_i I_r + V_r I_i \tag{4.9}$$

Equations 4.7 and 4.9 show that the computation of the active or reactive power from the real and imaginary components of the phasors involves two multiplications and one addition. These operations can be implemented with a microcomputer. A microprocessor with built-in hardware multiplier is preferred.

4.4.5 Computation of Power Factor

The power factor is defined as the cosine of the angle between the voltage and current phasors. The sign of the power factor is determined by the relative phase angle between the voltage and current phasors. If the current lags the voltage the power factor is +ve and if the current leads the voltage the power factor is -ve. Once the rms values of the voltage and current phasors and the active power are known, the power factor can be computed by using the following equation:

$$Power\ Factor = \cos\phi = \frac{Active\ Power}{V_{rms} I_{rms}} \tag{4.10}$$

The sign (lag +ve or lead -ve) can be determined from the sign of the reactive power. For lagging p.f. the reactive power is +ve and vice versa.

4.4.6 Computation of Energy

Active and reactive energies can be computed by integrating over time the values of active and reactive powers respectively. For achieving this on a microcomputer a hardware timer is required. Using known intervals of time, the values of active and reactive powers can be accumulated and scaled to yield the energy values in the required units.

4.4.7 Timing Considerations

In the EORW algorithm a specified number of consecutive samples (e.g. eight) are used to evaluate the real and imaginary components of the phasors representing the input signals. The time available between samples, assuming that the frequency of the inputs ranges from 55 - 65 Hz and a sampling rate of eight samples/cycle used, is 1900 μsec to 2275 μsec. Using eight samples per cycle is preferred because it facilitates performing the correlation with the input signal using inexpensive 8-bit microprocessors. The correlation functions can be represented using one byte each, for example, the binary number 11110000 can represent the odd function and the binary number 11000011 can represent the even function.

There are six input signals, one voltage signal and one current signal for each of the three phases. The total number of computations and control functions to be performed can be listed as follows:

(a) Digitization of six input signals,

(b) Implementation of the EORW algorithm for each signal,

(c) Computation of the rms value for each signal,

(d) Computations of the active and reactive powers for each phase,

(e) Computation of the power factor for each phase,

(f) Computation of the energy for each phase, and

(g) Determination of the frequency.

For maximum accuracy and rapid response to changes, the algorithm should be implemented such that the newest sample displaces the oldest sample and all the required computations described above are completed in the time available between the samples. In this case, the computations that are required to implement these functions are substantial and, therefore, a large and expensive computer facility would be required.

In this application a less expensive computing system for performing the computations has been considered. In this system two microprocessors are used to share the total computation load. The digitization of the input signals and the computations are

performed at the same time. The time required to complete the computations is approximately 6 milliseconds which is nearly half a cycle of the fundamental frequency. The algorithm uses eight consecutive samples and is evaluated every half cycle of the fundamental frequency. For each computation the four oldest samples, which represent the samples in a half cycle, are displaced by the four newest samples. After the first processor has completed its share of computations it transfers intermediate results to the second processor which completes the rest of the computations.

In this approach even though the computations are performed every half cycle, all the samples are used for evaluation of the phasor values of input signals. Therefore the accuracy of the phasors computed is not sacrificed.

4.5 Hardware Considerations

This section describes hardware considerations required for designing the system. In general, the hardware shall perform the following major functions:

1. Filter the unwanted components from the input signal.
2. Convert the input analog signal into digital data for processing by the microcomputer.
3. Provide a means to synchronize the sampling frequency with the frequency of the incoming signal.
4. Communicate with the user for input and output.

The following sections describe details of the hardware implementation.

4.5.1 Analog Filters

Analog filters are included in the instrument for eliminating high frequency components from the input analog signal. This is required because the instrument is meant to measure the power system parameters only at the fundamental frequency. Also, according to the sampling theorem, in order to reconstruct the signal accurately from the digitized samples, the sampling frequency must be greater than twice the highest frequency component present in the analog signal. Therefore analog filters should be

designed to attenuate all the frequency components other than the fundamental.

From the frequency response of the EORW algorithm shown in Figure 4.1, it is seen that the algorithm acts as an efficient filter and rejects all the even harmonics present in the input signal. Therefore, while designing the filter to attenuate unwanted components of the signal, the 2nd harmonic need not be considered. Also the presence of the second harmonic component will not lead to aliasing problem when the sampling rate is eight samples per cycle.

4.5.2 Digitization Unit

The function of the digitization unit is to convert the analog input signal to discreet values and to send the digitized values to the microprocessor. The principal constraints for the digitization process are the timing and the accuracy. Since one of the requirements is the measurement of the phase angle between the voltage and current phasors, the voltage and current signals from the same phase should be digitized simultaneously. Two possible ways to achieve this are illustrated in the block diagrams in Figure 4.3 and Figure 4.4.

In the system illustrated in Figure 4.3, the input signals are tracked continuously with separate sample and hold (S/H) units. The use of a S/H unit is essential because the input signal to the analog to digital converter must be constant during the time when the conversion is in progress. At the sampling instant, the six signals are held in response to a control signal from the microcomputer. Subsequently, a multiplexer selects one signal at a time and routes it to the analog to digital converter for digitization. The S/H units are returned to the sample mode after all the signals have been digitized. This procedure digitizes all the input signals at the same instant as the hold strobe to all the S/H units are given at the same instant.

In the second system shown in Figure 4.4, the input signals are divided into two groups. One group contains the three voltage signals and the other contains the three current signals. Signals of one group are routed to one multiplexer while the signals of other group are routed to another multiplexer. Each multiplexer is connected to a

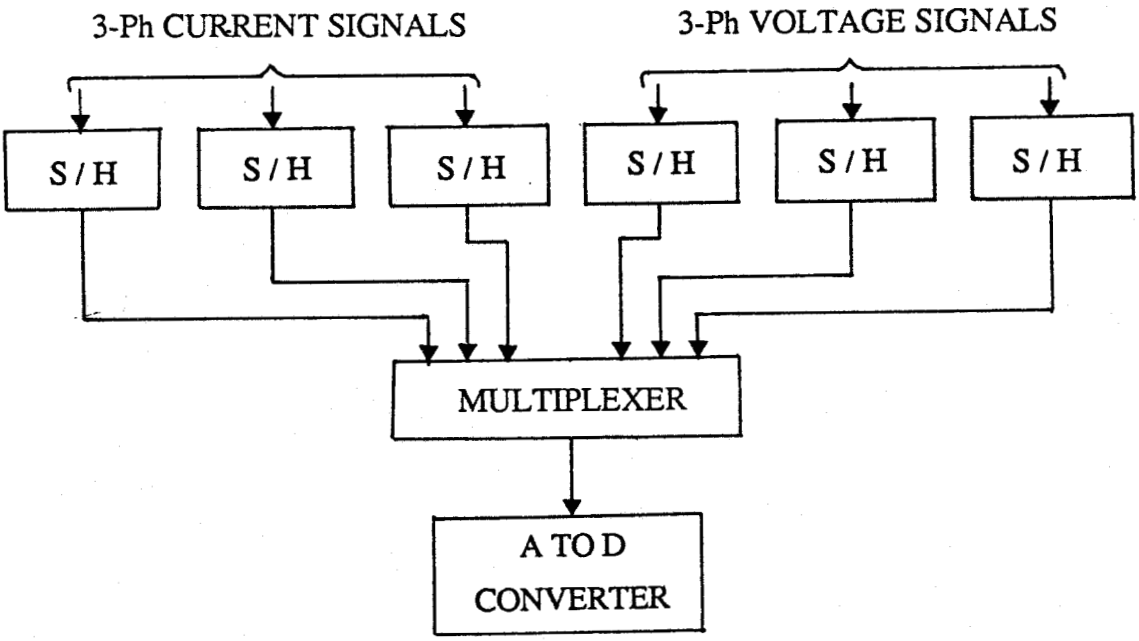

Figure 4.3. Digitization Unit Block Diagram I.

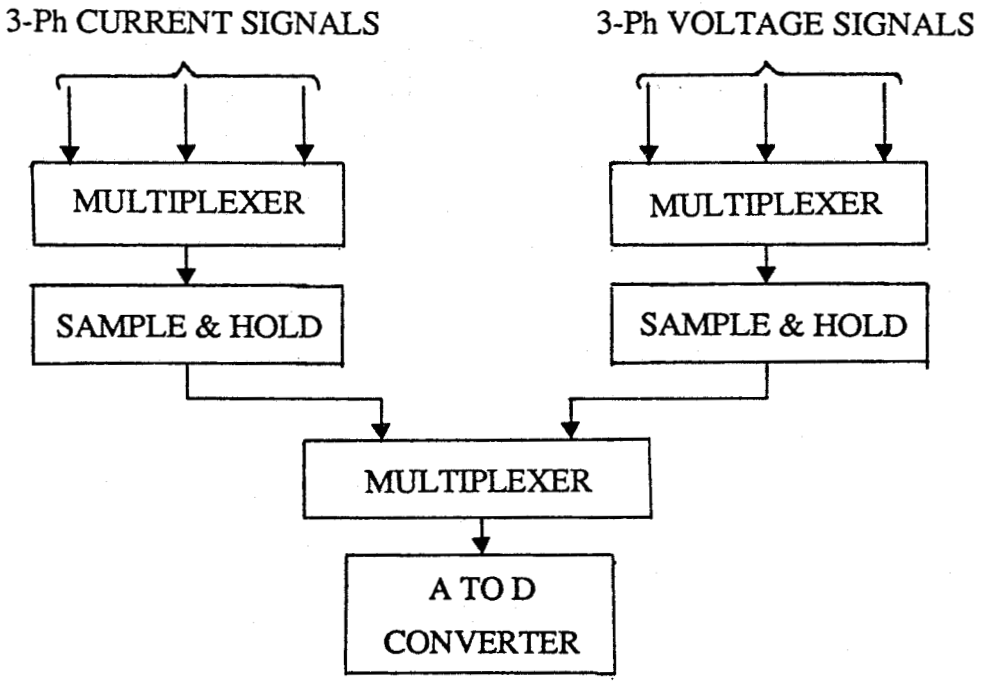

Figure 4.4. Digitization Unit Block Diagram II.

separate S/H unit. The two outputs from S/H units are subsequently multiplexed and routed to the analog to digital converter. In operation the first two multiplexers select a current and voltage signal from the same phase. These two signals are then sampled simultaneously and digitized subsequently.

Both of these approaches would be suitable for this instrument. In the first approach, the number of S/H units required is significantly larger than that required in the second approach. The second approach uses fewer components, although it would be difficult by this approach to determine the angle between the phases. But here in this application the angle between the phases is neither to be measured nor to be used in any computations as only the parameters of individual phases are required.

4.5.2.1 Analog to Digital Converter Selection

For the selection of the analog to digital converter (ADC), two main factors were considered : the resolution of the ADC and the conversion time.

The resolution, which is determined by the number of bits in the converted data, influences the accuracy of the conversion. Table 4.1 lists the maximum error due to the resolution limits in analog to digital conversion depending on the number of bits in the converted data (assuming a resolution of ± 1 LSB).

Table 4.1 : Error in analog to digital conversion due to resolution.

Number of Bits in the ADC	Percentage Error
8 - Bits	0.787
10 - Bits	0.195
12 - Bits	0.048
16 - Bits	0.0031

The requirement in this application is that the total error in the measurements of the parameters should not exceed one percent. The digitized values of the signals are used, directly or indirectly, for the computations performed in this instrument. Therefore, the error due to the ADC should be small. Also, other researchers have found [22] that the errors in computations of peak values and other parameters is adversely affected by the error in the analog to digital conversion. Therefore, among the ADCs listed in Table 4.1, a 12-bit ADC was selected for application in this instrument.

The second important consideration is the conversion time of the ADC. As discussed earlier, the overall processing time is one of the important factors in the system design for this application. Since the number of conversions required is approximately 2880 (480 × 6) conversions per second, and a number of other computations are to be performed, an analog to digital converter with 25 μsec conversion time was chosen.

4.5.3 Microcomputer Selection

As discussed in the earlier sections, the processing time is one of the important considerations in the design of this instrument. The measurement of so many parameters makes the instrumentation task computationally intensive. In order for the software to be executed in a reasonable length of time as stipulated by the time calculations in Section 4.4.7, the hardware must be optimized for the task. The factors that influenced the choice of the hardware are as follows:

1. The project must use the development support that already exists in the research facility.
2. A commercially available single board computer should be used to reduce the hardware development time.
3. The processor must support the instructions suitable to the software requirements.

It was decided that the system microcomputer would use an Intel microprocessor. This choice was based primarily on the development support available in the research facilities of the Department of Electrical Engineering (Intel Series IV Development System) [23,24].

Based on the factors discussed above, the two microprocessors that are appropriate for this project are the Intel 8051/8052 microcontroller [25] and iAPX86 microprocessor [26]. The iAPX prefix refers to the Intel Advanced Processor line of products. Some of the salient features of the two processors are listed below.

The main features of the Intel 8086 microprocessor are:

- HMOS technology,
- 1 Megabyte memory address space,
- 16-bit internal and external data bus,
- 16-bit internal registers,
- 8 and 16 bit signed and unsigned arithmetic,
- 5, 8 and 10 MHz clock rates,
- instruction prefetch queue,
- segmented memory with segments up to 64 Kbytes long,
- access to words on even or odd boundaries,
- special instructions for string operations such as move string, compare string, load string from memory, store string to memory, and
- separate memory and I/O address space.

The main features of the 8051/8052 microcontrollers are as follows:

- HMOS technology,
- 8-bit CPU,
- 128-bytes of on-chip data memory (256-bytes on 8052),
- On-Chip oscillator and clock circuitry,
- 32 I/O lines,
- 64K address space for external data memory,

- 64K address space for external program memory,
- Two 16-bit timers/counters (three on 8032/8052),
- A five-source interrupt structure (six sources on 8032/8052) with two priority levels,
- Full duplex serial port,
- Boolean processor, and
- 12 MHz operation (requires minimum 12-cycles per instruction).

A comparison was made on the basis of the time taken to execute the algorithms and the components required in the microcomputer system for the two processors. The execution time for a selection of algorithms is listed in Table 4.2.

Table 4.2 : Algorithm execution time using the 8051 and 8086 microprocessors.

Software	Execution Time μs	
	8051	8086
1. EORW Algorithm Implementation	150	115
2. Peak Value Computation	250	175
3. Power Computation	350	225

As discussed in Section 4.4.7, the time available for one set of calculations is approximately 7 milliseconds. The execution time required by the 8086 microprocessor is less than that required by 8051 microcontroller. The total time considering all the computations for the three phases, namely, digitization time, display time, overhead time etc. showed that neither of the two processors can complete the computations in 7 milliseconds available for performing the computations. Therefore, two processors, of this variety, working in parallel, are required to complete the measurement task. The decision was made in favour of using the 8051/8052 microcontrollers for the following

reasons:

1. Less extra hardware would be required as the microcontroller has on chip timers/counters, serial port, parallel ports and memory.
2. The 8051 microcontroller chip is less expensive than the 8086.
3. Though the processor has 8-bit data bus, the computations can be performed in double precision for 16-bit operations, if required. (The timings given in Table 4.2 are for double precision arithmetic).
4. Several single board computers based on 8051/8052 microcontrollers are commercially available.

Details of 8051/8052 architecture are given in Appendix A.

4.5.4 Display Design

The output of the instrument is to be displayed in a digital format. There are at least two different ways of achieving this . The data could be displayed with seven-segment light emitting diodes (LEDs) or with a dot matrix display unit. Alternatively the data could be displayed on a video display terminal.

In the former case the data which are in the binary format must be converted into a BCD (binary coded decimal) format, latched, and transferred to seven-segment LED drivers. Since a minimum of four seven-segment LED's are needed to display each parameter and 7 parameters are to be displayed for each phase, the total number of seven segment LED's required can be calculated as follows:

$$\textit{Total no. of 7-segment LED's required} = 4 \times 7 \times 3$$
$$= 84$$

The conversion of data from binary to BCD format could be done either by dedicated hardware or by software. The available binary to BCD converters convert a maximum of 6-bits of binary to BCD. The hardware for converting 16-bit binary to BCD would require 16 of these 6-bit binary to BCD converters. The cost and complexity of such a unit would be high. It might also be required to convert a binary number which is more than 16-bits long.

Using software to convert binary to BCD is another alternative. The main drawback of this method is that the conversion process consumes a lot of processor time.

A compromise was made between the cost and complexity of the system and response time of the system. A custom made single board microcontroller card, BCC-52, was used. This is a microcontroller that is based upon Intel 8052, and has a BASIC interpreter built into it. This microcontroller can be directly interfaced to a suitable video monitor. This microcontroller can be programmed in BASIC-52 language (which is a subset of BASIC language) and can be made to display the results on the monitor screen in the desired digital format. The details of the board are discussed in a succeeding section.

4.5.5 Frequency Measurement and Control

For the purpose of frequency measurement and control, a phase-locked loop circuit was used. As discussed in the Section 4.4.2, if the number of samples per cycle is constant then the errors due to a drift in the input signal frequency reduce considerably. To get a constant number of samples per cycle the sampling rate should be, directly or indirectly, controlled by the incoming signal frequency. To achieve this, one possible scheme consists of multiplying the incoming signal frequency by a large factor (say 2000) and then sampling the signal after a fixed count of the multiplied frequency has elapsed. Multiplication by a large factor is important because the power system frequencies are very small (near 60 Hz) compared to the timer clock frequency. If the pulses of high frequency are counted then the time resolution of the count increases and thus the accuracy of the sampling rate will be improved. The multiplication of the input signal frequency can be done using a phase locked loop and a frequency divider circuit. The details of the design are given in a later section.

Frequency measurement is another function that can be performed from this frequency control scheme. The time taken to count a fixed number of pulses of the frequency multiplier output can be determined using a timer which runs at a fixed clock rate. Using this time value, the frequency of the incoming signal can be computed.

Another method, which was used in this design, is to use a look up table and use the count in the timer to address the current frequency value. The details of the actual operation are discussed in a succeeding section.

4.6 System Components

4.6.1 The Prototype System

Figure 4.5 shows the block diagram of the overall system. There are six input signals to the system, three voltages and three currents, one for each phase.

It is assumed that the voltage signals are scaled down to 2.5 volts, for the rated voltage, using potential transformers. It is also assumed that the current signals are first scaled using current transformers and then converted into voltage signals so that the rated current is represented by 2.5 volts. These scaled voltage signals act as inputs to the instrument. All input signals are then passed through individual analog filters to attenuate the non-fundamental frequency components.

After filtering, the signals are digitized consecutively in the digitizer as discussed in the Section 4.5.2. The microcomputer stores the digitized values in the memory and evaluates the parameters from the samples. The result is displayed on the video monitor. The sampling is controlled by the output pulses from the phase locked loop which multiplies the incoming signal frequency by a fixed factor of 2000. The composition of each of the components is discussed in this section.

4.6.2 Analog Filters

The analog filter unit consists of six switched capacitor 6th order Butterworth filters [27]. The operation of a switched-capacitor filter is based on the ability of on chip capacitors and MOS switches to simulate resistors. The value of the resistor is dependent on two quantities : the capacitor value which is fixed and the switching rate which can be varied. Thus the value of R is adjustable by adjusting the clock frequency, which controls the switching rate. There are many advantages of using switched capacitor filters over

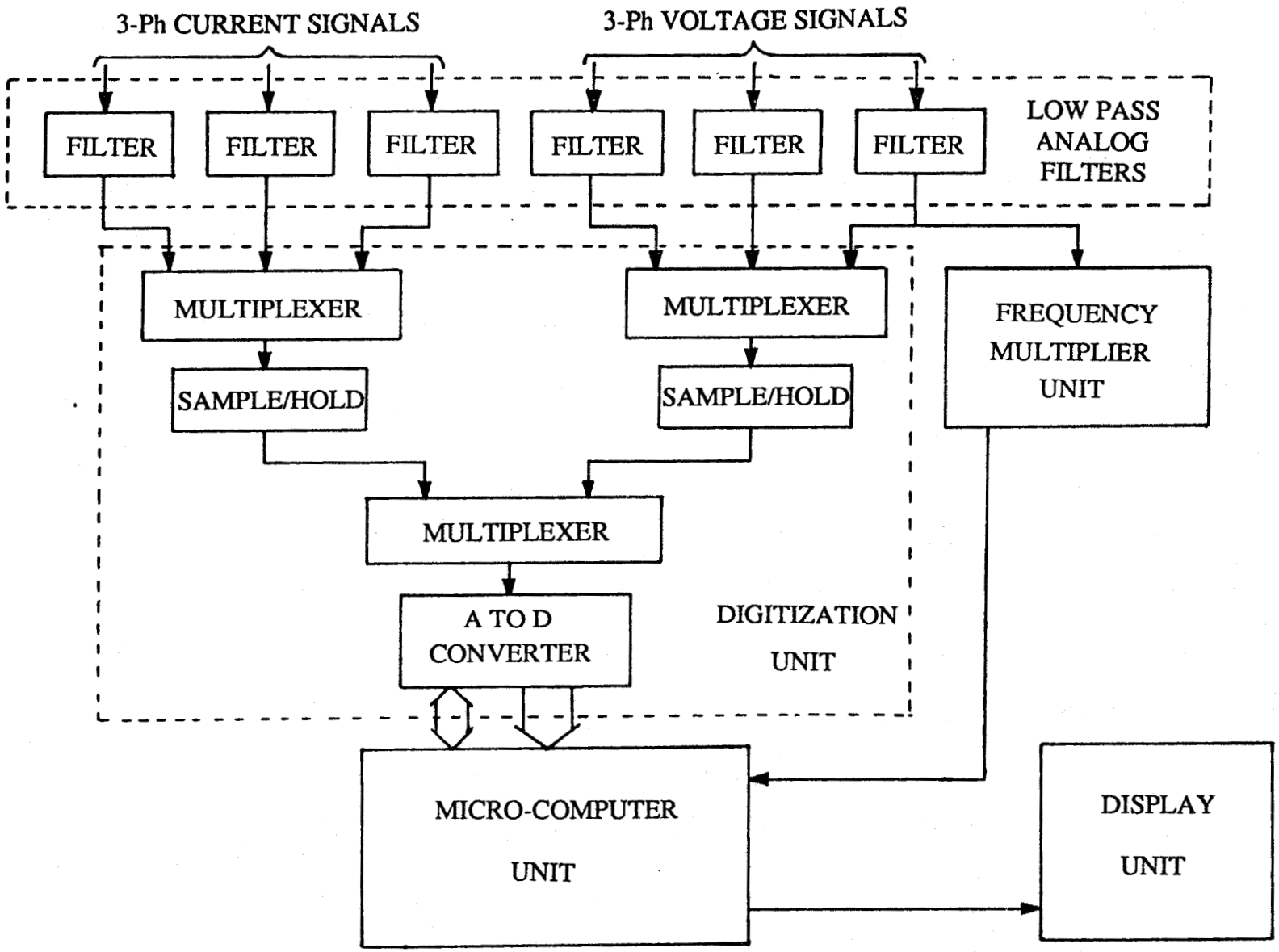

Figure 4.5. Block Diagram of Complete System.

conventional passive or active filters. Switched capacitor filters need no external capacitors or inductors and their cutoff frequencies are set to a typical accuracy of ±0.3% by an external clock frequency. In addition, switched capacitor filters have very low sensitivity to temperature changes.

Some of the main features of the 6th order switched capacitor Butterworth filter (product no. MF6 [27]) are:

- No external components,
- Cutoff frequency accuracy of ±0.3%,
- Two uncommitted op amps available,
- 5V to 14V operation,
- Cutoff frequency set by external/internal clock.
- 14 -pin DIP,
- Low cost,
- Easy to use,

The circuit diagram and design details are given in Appendix D.

4.6.3 The Digitizer

As discussed earlier, the digitizer consists of an analog to digital converter, two sample and hold circuits and three multiplexers. The analog to digital converter chosen is a 12-bit successive approximation type with a conversion time of 25 μs. The components chosen for use in the digitization unit are listed in Table 4.3.

Some of the important specifications of the S/H unit, Multiplexer and Analog to digital converter are listed in Tables 4.4, 4.5 and 4.6. Detailed specifications are given in Appendix E.

The chosen sample and hold unit has a maximum drift rate of 5 mV/s and a maximum acquisition time of 6 μs. The drift rate is important because the value of the voltage and current of the same phase must be held fixed for the entire duration of the conversion of the two signals. The acquisition time of S/H unit should also be low (6 μs

Table 4.3 : Components used in Digitization Unit.

Function	Component
Sample & Hold	INTERSIL - IH5110
Multiplexer	SCL4052B
A to D converter	HARRIS - HI574A

Table 4.4 : Specifications of Sample and Hold Unit [28].

Intersil - IH5110 Sample & Hold		
Parameter	Value (max.)	Units
Acquisition time for max. Analog Voltage Step	6	μs
Drift Rate	5	mV/s
Input Impedance in Hold or Sample mode	100	MΩ

in this case) because after analog to digital conversion for one phase the signal for the next phase should be acquired fast in order to avoid any delay.

The output impedance of the multiplexer is 580 ohms and the signal source to the analog to digital converter should have a low impedance of the order of 1-4 ohms. To meet this requirement, a low output impedance (2 ohms) and high input impedance unity gain buffer (LM 103) [31] has been used between the output of the multiplexer and the input of the analog to digital converter. The circuit diagram of the digitization unit is given in Appendix F.

Table 4.5 : Specifications of Multiplexer [29].

SCL4052B - Multiplexer		
Parameter	Value(max.)	Units
On - Resistance	580	Ω
Propagation Delay Time	60	ns
Bandwidth (-3dB)	40	MHz

Table 4.6 : Specifications of Analog to Digital Converter[30].

HARRIS - HI-574A A to D Converter		
Parameter	Value (max.)	Unit
Resolution	12	Bits
Linearity Error	± ½	LSB
Analog Inputs	-5 to +5 -10 to +10 0 to +10 0 to +20	Volts
Input Impedance (10 V span)	5K ± 25%	Ohms

4.6.4 The Microcomputer

As discussed earlier, the microcomputer consists of two processors operating in parallel. The two processors chosen are Intel microcontrollers 8031 and BASIC-52 (8052 with built in BASIC interpreter in it). The single board microcomputers which use these

processors are FX-31 (based on Intel 8031) [32] and BCC-52 (based on Intel BASIC-52) [33].

4.6.4.1 FX-31 Single Board Computer

Allen System's FX-31 Computer Board is a general purpose single board computer utilizing Intel's 8031 microcomputer [25]. Much of the board's capability results directly from the 8031. This 40 pin DIP IC has a full duplex Universal Asynchronous Receiver Transmitter.

A standard 6.5 inch length by 4.5 inch width board size is incorporated into the design. A 22/44 pin standard finger connector allows the necessary lines to be brought out over a 44 connector bus (non-standard). Additionally, a 40-pin connector is employed on the board to provide easy access to the board's four parallel ports, TTL serial lines and RS-232C serial lines. Besides the microcontroller, address/data latch, and the address decoder, the board has provision for the following components:

- I/O expansion chip (8255) which provides 3 additional 8-bit I/O ports,
- 16 Kbytes of EPROM space (if two 8 Kbyte EPROMs are used),
- 16 Kbytes of RAM/EPROM space (If 8 Kbyte units are used).

4.6.4.2 BCC-52 Single Board Computer

The BCC-52 computer is a single board controller/development system. The BCC-52's 17 chip circuit is housed on a compact 6.5 by 4.5 inches board. It contains RAM/EPROM, an EPROM programmer, 3 parallel ports, and 2 serial ports.

The computer is based on the 8052AH-BASIC chip which is the programmed version of the INTEL 8052 microcontroller. The 8052AH contains 8K bytes of on-chip ROM, 256 bytes of RAM, three 16-bit timers/counters, 6 interrupts and 32 I/O lines. In the 8052AH-BASIC the ROM is a masked BASIC interpreter and the I/O lines are redefined to address, data, and control lines.

The BCC-52 contains an 8255 PIA which provides three 8-bit input/output software configurable parallel ports. There are two serial ports on BCC-52 board; one for the

console I/O terminal and the other for an auxiliary serial output port, frequently referred to as the line printer port. When using an 11.0592 MHz crystal, the console port does auto baud rate determination on power up.

One of the unique and powerful features of the BCC-52 is that it has the ability to execute and save programs in an EPROM. The 8052AH chip actually generates all the timing signals needed to program 2764/128 EPROMs. Unlike most EPROM programmers that fill the entire contents of an EPROM regardless of the application program size, BCC-52 treats the EPROM as "write once mass storage". That is when a program is saved on EPROM, it is tagged with an identifying number and stored only in the amount of EPROM required to fit the program. Additional programs can be stored on the same EPROM, if space is available, and they are tagged with different identifying numbers. A detailed description of the BCC-52 microcomputer board is given in Appendix B.

4.6.5 Phase Locked Loop

In order to have a fixed number of samples per cycle and to perform frequency measurement, a phase locked loop circuit has been used. The main function of this phase locked loop is to multiply the incoming signal frequency by a factor of 2000. The phase locked loop chosen here is a CMOS integrated circuit SCL 4046B [29]. It contains two phase comparators, a voltage controlled oscillator (VCO), a source follower and a zener diode. The block diagram of this phase locked loop circuit is illustrated in Figure 4.6.

The phase comparator I (an exclusive-OR gate) provides a digital error signal and maintains 90° phase shift at center frequency between the signal and comparator inputs (both at 50% duty cycle). Phase comparator II (with leading edge sensing logic) provides digital error signals and phase pulses, and maintains a 0° phase shift between the input signals (duty cycle is immaterial). The linear VCO produces an output signal VCO_{out} whose frequency is determined by the voltage of input VCO_{in} and capacitors and resistors C1,R1,C2,R2. The Zener diode can be used to assist in power supply regulation. Refer to circuit diagram in appendix E.

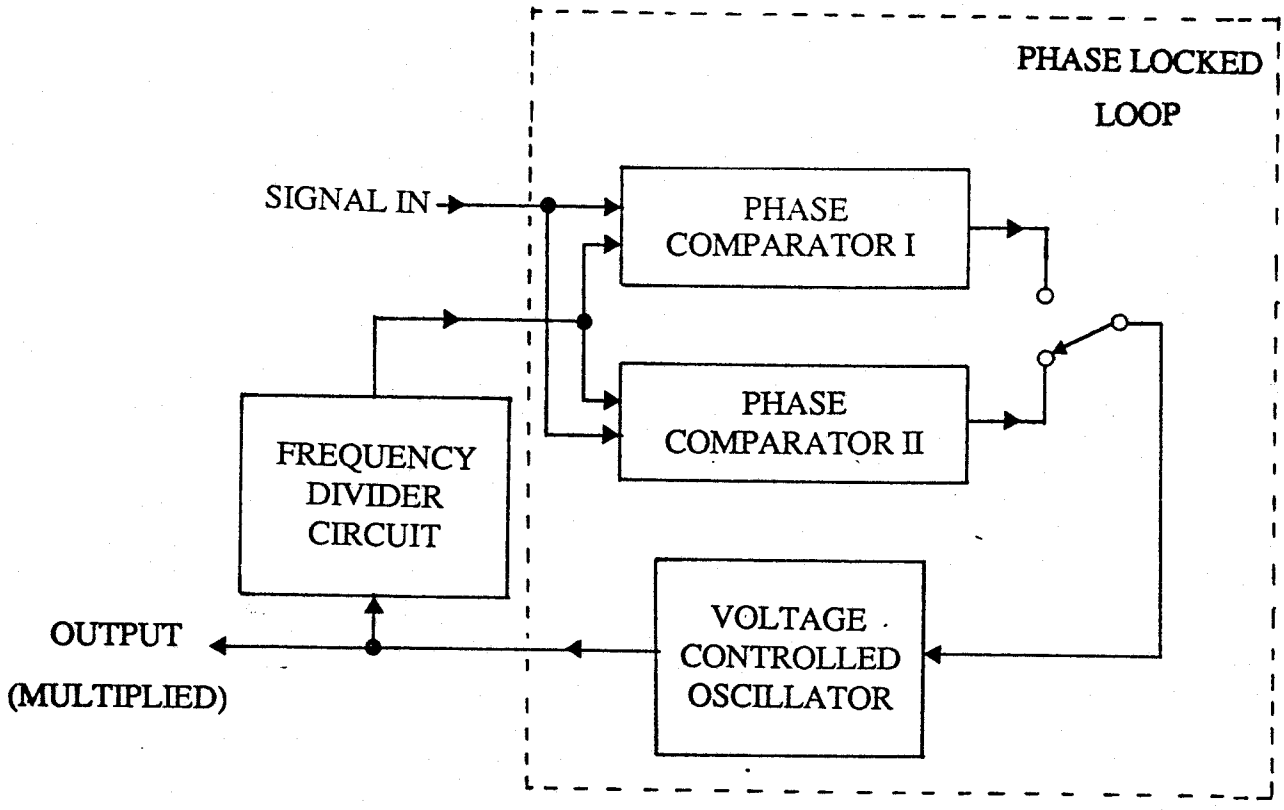

Figure 4.6. Block Diagram of Frequency Multiplier Unit.

The functional block diagram of the phase locked loop circuit used to multiply the incoming signal frequency by a factor of 2000 is shown in Figure 4.6. Because the available chip has a lower frequency limit of 100 Hz for accurate operation, the input signal frequency (approximately 60 Hz) was first multiplied by a factor of 2. This multiplication is achieved using a full wave rectifier. This signal is given as input to a Schmitt trigger [29]. The output of the Schmitt trigger is a rectangular wave of a frequency which is twice that of the incoming signal.

The output of the Schmitt trigger constitutes one of the inputs to the phase comparator. Here phase comparator I is not used because the 50% duty cycle constraint may not be satisfied as the triggering of the Schmitt trigger depends on the input signal level, which can vary.

The output of the VCO is connected to a frequency divider circuit configured to divide by a factor of 1000. The frequency divider circuit is designed using three decade

counters [29]. The output of this frequency divider is the other input to the phase comparator. Thus when the two inputs to the phase comparator are in phase, the frequency of the VCO output is 2000 times that of the incoming signal frequency.

4.6.6 The Display Unit

The display device used in this project is Qume video display terminal type QVT 101 [34]. It has a 14 inch screen with 24 lines by 80 character display. It is programmable to operate in various display modes. It is compatible with the EIA RS-232-C interface standard. Thus it can be directly interfaced with the single board microcomputer BCC-52 which has a RS-232-C serial port.

4.7 Concluding Remarks

In this chapter, the design of a microprocessor based instrument used to measure various parameters in a 3-phase power system is described. Specifications for the instrument were determined to assure performance compatible to existing instrumentation. Among various algorithms for the determination of phasor components of voltage and current signals, the Even and Odd Rectangular Wave algorithm was selected. These voltage and current phasors were then used to compute other parameters of the power system, namely, the rms values of voltages and currents, the active and reactive powers, the energies and the power factors. For the measurement of frequency a phase-locked-loop circuit along with a stable crystal oscillator was used. The system hardware consisted of analog filters, a digitization unit, a microcomputer unit, a frequency multiplier unit and a display unit.

Analog filters were used to reduce the noise and high frequency components from the input signals. A 12-bit successive approximation analog to digital converter was used to digitize the input signals. The microcomputer unit consisted of two single board microcomputers, based on Intel's 8051 and 8052 microcontrollers, operating in parallel. The SBC-8052 could be programmed in BASIC and could be directly interfaced with a video display terminal. The frequency multiplier unit consisted of a phase-locked-loop

circuit in a frequency multiplier configuration. The frequency multiplier unit was used for measurement of the frequency as well as to control the sampling rate to eight samples per cycle, irrespective of the input signal frequency. The display device used in the instrument was a video display terminal.

The implementation of the software and the operation of the system is described in the next chapter.

CHAPTER 5

IMPLEMENTATION AND OPERATION OF THE INSTRUMENT

5.1 Introduction

This chapter describes the operation of the instrument including the implementation of the system software. The subroutines of the software are discussed in detail. Also the organization of the data memory is described. The operation of the total system is discussed starting from the instant of switching the power on.

5.2 General

The tasks of controls and computations are shared between two single board micro-computers, an SBC-8051 and an SBC BASIC-52. As discussed in Section 4.4.7, the EORW algorithm is implemented so that the phasor values are updated every half cycle. The EORW algorithm uses the sampled values of the inputs and it is processed so that its computation is completed once in every half cycle.

The parameters such as the rms values of the voltages and currents, and the active and reactive powers must be computed using the components of the phasors representing the inputs during a given half cycle. The EORW algorithm, and the computation of these parameters are implemented on one single board micro-computer, SBC-8051. This micro-computer also acts as the master controller and sequences the digitization and data transfer between the two micro-computers. The number of computations to be performed in a half cycle i.e. about 7 ms., makes the software on the SBC-8051 time-critical.

The parameters such as energies, power factors and frequency, which are derived quantities, can be computed using the values of their parent parameters that have been averaged over several cycles. The computations of these parameters are implemented on the SBC BASIC-52. The SBC BASIC-52 also performs the scaling of the computed parameters and displays them on the monitor screen in a tabular format.

To optimize the processing time, the SBC-8051 is programmed using Assembly language. For programming the SBC BASIC-52, both BASIC and Assembly languages

are used. The formatting of the display (tabular format as shown in Appendix G) and the user inputs, and the computation of the scaling factors is done using the BASIC language. These functions are performed off-line. The other computations and scaling are programmed using the Assembly language. For computations in floating point arithmetic, various BASIC subroutines are called from the assembly language programs.

5.3 Software for the SBC-8051

The computation of the selected parameters requires substantial software. Therefore, the software was divided into a number of subroutines. Subroutines with defined input and output variables were first developed and were then included in the main program. The subroutines written for the SBC-8051 are:

- a subroutine for implementing the EORW algorithm,
- a subroutine for computing the active and reactive powers,
- a subroutine for performing 16×16 bit multiplication, and
- a subroutine for computing the rms values.

Details of the subroutines are discussed in the following sections.

5.3.1 EORW Algorithm Subroutine

The inputs are correlated with even and odd rectangular waves in this subroutine. Since the inputs are digitized 8-times per cycle, the correlation functions can be represented using one byte (8-bits) each. The odd function is represented by the binary number 11110000 and the even function is represented by the binary number 11000011 (a "1" represents addition and a "0" represents subtraction).

The algorithm is evaluated every half cycle, and, since there are eight samples in each cycle, it operates on four new samples at a time. For correlation with the odd function (11110000), four consecutive samples are added together, and the result is stored. Similarly, the next four consecutive samples are added together, and the result is stored as a negative quantity with a 2's complement representation. For correlation with the even function (11000011), 2 consecutive samples were added and the next two

consecutive samples were subtracted. Then the 5th and 6th samples were subtracted from the sum of 7th and 8th samples. The results of these operations are stored in separate memory words (a memory word consists of two bytes).

During the operation of the algorithm the accumulated four newest samples are added together and this result replaces the result of a previous addition. The procedure for successive calculation of the real component (using even correlation) is illustrated below.

Assume that $S_{-8},S_{-7},.....,S_{-1}$ are eight consecutive samples (*old*) and $S_1,S_2,.....,S_8$ are eight consecutive samples (*new*). For the purpose of correlation the four quantities, given below, are calculated from the samples. These quantities are stored in four separate memory locations (words). The contents of these four memory words are, $(S_{-8}+S_{-7}+S_{-6}+S_{-5})$, $-(S_{-4}+S_{-3}+S_{-2}+S_{-1})$, $(S_1+S_2+S_3+S_4)$, and $-(S_5+S_6+S_7+S_8)$ respectively.

These four results can be named as $S_{old-1}, S_{old}, S_{new}, S_{new+1}$ respectively. The process of updating the real component, RE, of the input signal, at any instant of time, is as follows:

$$RE_{new} = RE_{old} - S_{old-1} + S_{new} \tag{5.1}$$

$$RE_{new+1} = RE_{new} - S_{old} + S_{new+1} \tag{5.2}$$

This value of the real component is scaled by a scaling factor A which is dependent on the number of samples in the data window. For a data window of eight samples and a sampling rate of 480 samples per second, the scaling factor A can be determined using Equations 3.29 and 3.30.

Assume that the input signal is a *sine* wave of $1.0\,p.u.$ peak value. The real and imaginary components are calculated using Equations 3.29 and 3.30 that are reproduced

below.

$$v_r = (\frac{1}{A}) \sum_{n=0}^{m-1} v_{k+n-m+1}\, signum \left\{ sin\,(\frac{2\pi n}{m}) \right\} \tag{5.3}$$

$$v_i = (\frac{1}{A}) \sum_{n=0}^{m-1} v_{k+n-m+1}\, signum \left\{ cos\,(\frac{2\pi n}{m}) \right\}. \tag{5.4}$$

In these equations $m = 8$. Thus, the real and imaginary components can be computed as follows:

$$\begin{aligned} v_r = (\frac{1}{A})\,(sin\ 0 + \sin\frac{\pi}{4} + \sin\frac{\pi}{2} + \sin\frac{3\pi}{4} \\ - \sin\pi - \sin\frac{5\pi}{4} - \sin\frac{3\pi}{2} - \sin\frac{7\pi}{4}) \\ = (\frac{1}{A})\,4.82 \end{aligned} \tag{5.5}$$

$$\begin{aligned} v_i = (\frac{1}{A})\,(sin\ 0 + \sin\frac{\pi}{4} - \sin\frac{\pi}{2} - \sin\frac{3\pi}{4} - \sin\pi \\ - \sin\frac{5\pi}{4} + \sin\frac{3\pi}{2} + \sin\frac{7\pi}{4}) \\ = (\frac{1}{A})\,2.0 \end{aligned} \tag{5.6}$$

The peak value calculated from v_r and v_i is

$$\frac{1}{A}\sqrt{(4.82)^2 + (2)^2} = 5.22625\ \frac{1}{A}$$

Therefore,

$$A = 5.22625 \tag{5.7}$$

A similar technique is used for evaluation of the imaginary components of the input signals using the even function. To obtain the initial values of the real and imaginary components, the old values of samples and the real and imaginary components are assumed to be zero.

The real and imaginary components as computed above are 16-bit quantities. This is because a 12-bit ADC is used and 8-samples are used for determining the real and imaginary components. Therefore, all computations must be performed using double precision arithmetic in order to avoid truncations.

5.3.2 Power Subroutine

For computing the active and reactive powers, Equations 4.7 and 4.9 are implemented in the Power Subroutine. The real and imaginary components of the voltages and currents are 16-bit quantities. Therefore, for the multiplications in Equations 4.7 and 4.9, a 16 bit multiplication routine is used. Active and reactive power computations each require two 16-bit multiplications and one addition or subtraction.

5.3.3 16-Bit Multiplication Routine

A 16 bit multiplication routine is implemented using the 8-bit unsigned multiply instruction available in the 8051 microprocessor instruction set. This instruction multiplies the 8-bit numbers in the accumulator and register B, and the 16-bit result is returned to the accumulator (high byte) and the register B (low byte). The instruction

does not distinguish between the signs of the numbers and assumes the numbers to be positive.

In the subroutine, the signs of the two 16-bit numbers to be multiplied are checked first and a flag is set if the result is to be a negative number. Then the negative number(s), if any, is(are) converted into a positive number(s) with the 2's complement method. These two positive 16-bit numbers are multiplied using the 8-bit multiplication instruction. The multiplication procedure is illustrated in Figure 5.1.

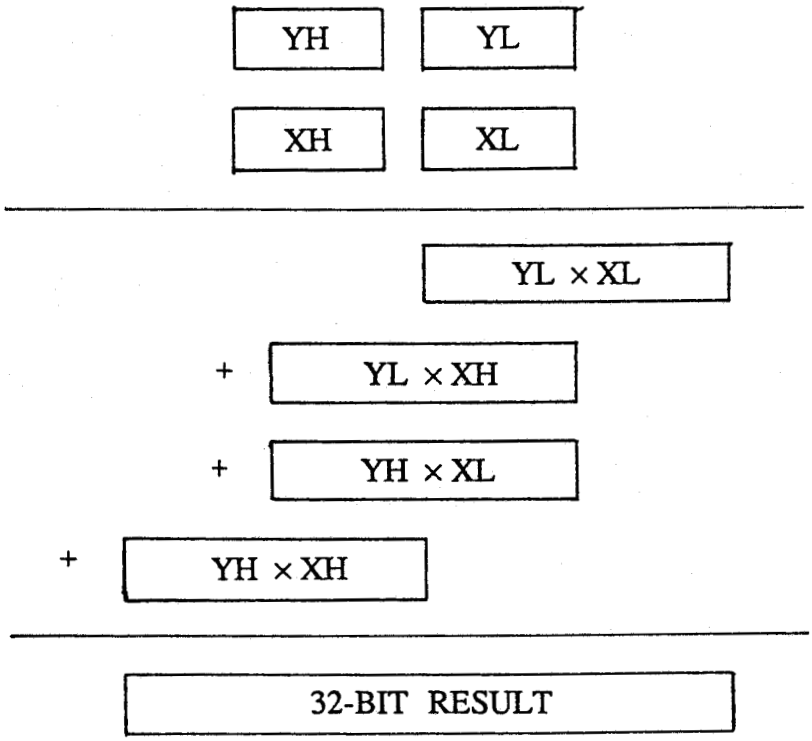

Figure 5.1. 16-bit Multiplication Procedure.

1. Multiply the low bytes XL and YL and store in Z1 (16-bit).
2. Multiply the low byte YL with the high byte XH. Shift left the result Z2 by a byte.
3. Multiply the high byte YH by the low byte XL. Shift left the result Z3 by a byte.
4. Multiply the high bytes XH and YH. Shift left the result Z4 by 16-bits.

5. Add Z1, Z2, Z3, and Z4 to give the final result which is 32-bit long.

After this 32 bit result is obtained, the sign flag is tested and if set, the result is converted into negative number by the 2's complement method.

5.3.4 RMS Value Computation Subroutine

For computing the rms value of a voltage (or current), the real and imaginary components of the voltage (or current) phasor are used. As described earlier, for the implementation of this subroutine, Piecewise Linear Approximation technique (described in Appendix C) is used. The rms value can be approximated by the following equation:

$$P = x_n \cdot a + y_n \cdot b \tag{5.8}$$

where

a = max (|re|, |im|),

b = min (|re|, |im|),

and x_n, y_n are coefficients for nth region in which the fraction b/a lies.

Here a four region approximation is used. The mean value of the error for a four region approximation is 1.3972×10^{-4}. The coefficients for the four regions are given in Table 5.1.

For the implementation of the rms value subroutine, a comparison between the values of a and b is made to find out the region in which the fraction b/a lies. Then the rms value is computed by multiplying the real and imaginary components of the signal by the coefficients from the respective region. Since the coefficients are fractional values, the multiplication is done by shift and add approach.

5.3.5 Data Memory Organization

The 8051 microcontroller contains 128 bytes of on-chip random access memory (RAM). Also, 64 Kbytes of external RAM can be interfaced to it. The time taken by the processor to access external memory is twice the time taken to access the on-chip

Table 5.1 : Four-region coefficients for calculating peak values.

Region	x	y
$0 = b/a \leq 0.25$	0.9951	0.1234
$0.25 < b/a \leq 0.50$	0.9392	0.3497
$0.50 < b/a \leq 0.75$	0.8506	0.5286
$0.75 < b/a \leq 1.00$	0.7547	0.6574

memory. Also, the external memory can be accessed only through the accumulator. The data memory is organized in this application so as to reduce the processing time.

The on-chip memory is used to store the digitized samples obtained from the digitizer. As mentioned earlier, two memory banks are required to store the digitized values. These memory banks (24 bytes each) are created at locations 20H to 37H, and 40H to 57H respectively. The variables used in different subroutines are also stored in this RAM. Figure 5.2 shows the organization of the on-chip RAM. Before the execution of a subroutine, the variables for the subroutine are transferred from the external RAM to the internal RAM and after the execution of the subroutine the results are transferred back to the external RAM. A register bank (8-bytes) and the stack for the processor operation are also located in the on-chip RAM.

The external RAM is used to store the values of the parameters obtained from the subroutines. Since the same parameters are to be computed for the three phases, the concept of paging is used for ease of operation. The parameters of one phase are stored in one page of external memory (one page of memory consists of 256 bytes). In the 8051 processor, the external memory is addressed through port-0 (low byte) and port-2 (high byte). Paging can be achieved by addressing the page numbers through port-2 and addressing within the page through port-0. Thus three pages of external RAM are used

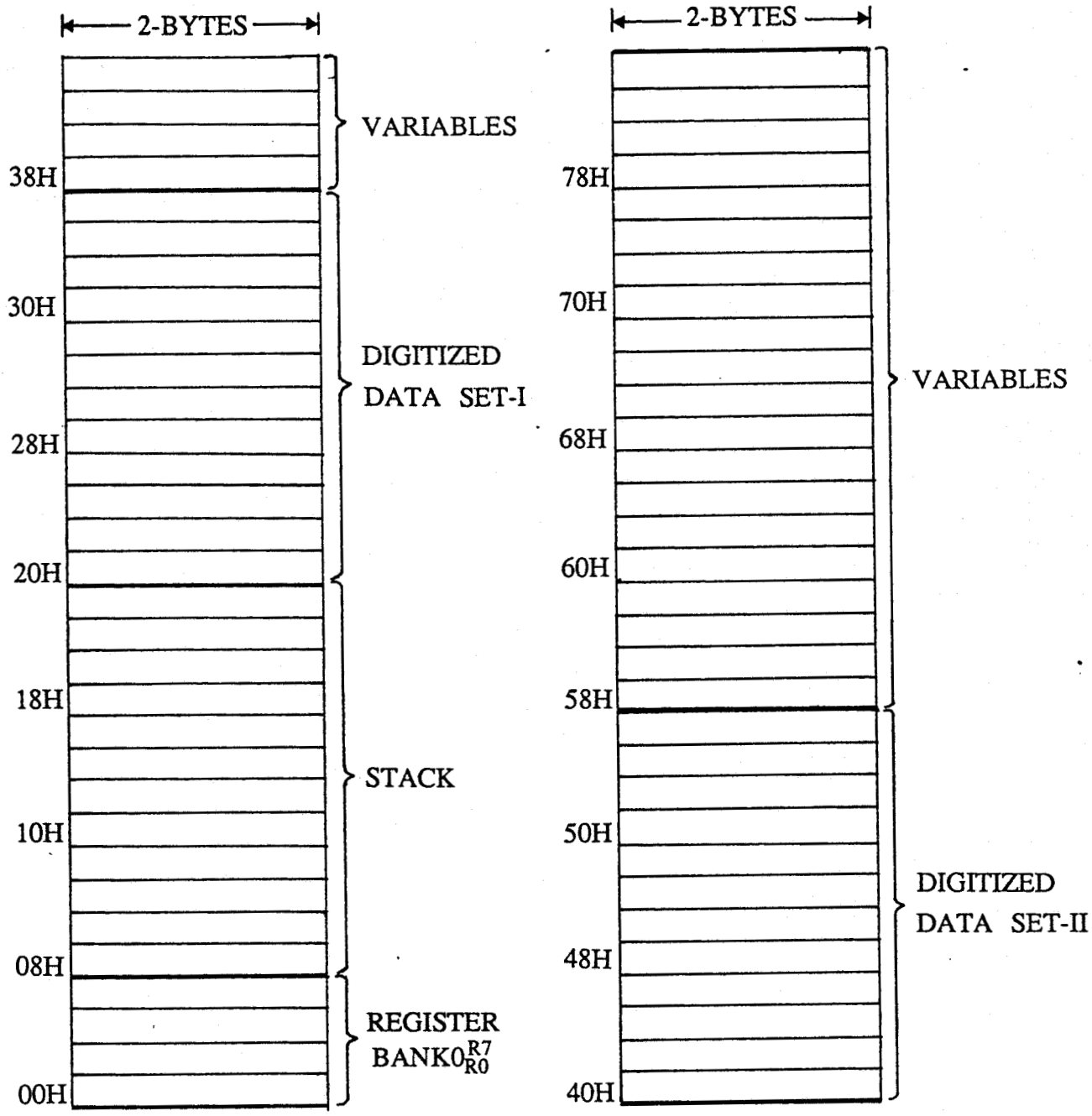

Figure 5.2. Internal Data Memory Maps.

for storing the parameters of the three phases.

A small program is written to call the different subroutines for computing the parameters of one phase. The same routine is called thrice, once for each phase. Before calling this routine the address at port-2 is changed to point to the page of memory corresponding to the phase whose data is to be processed.

5.4 Software for the SBC BASIC-52

The software for the SBC-8052 is written using both the BASIC and Assembly languages. A portion of the program is written in BASIC for off-line computation and display. A number of subroutines are written in assembly language for the scaling of voltages, currents, and active and reactive powers and for the computation and scaling of energies, power factors and frequency. For computations in floating point arithmetic, various BASIC subroutines are called from the assembly language programs.

For scaling voltage, current and power, the values transferred from the SBC-8051 are multiplied by the respective scaling factors. For the computation of the energies, the accumulated values of power are added together, integrated with respect to time and scaled. The power factor is computed using the values of voltage, current and active power. For the evaluation of frequency, the timer data transferred from SBC-8051 is used and the correct value of the frequency is displayed from a look-up table based on the timer data.

5.5 System Operation

When the system is powered up, both processors start executing programs stored in their respective EPROMs, starting from location 0000H. The 8051 processor first initializes all the special function registers viz., timer/counter mode control register, timer/counter control register, interrupt enable control register, interrupt priority control register, timer 0 and timer 1 registers etc. It also configures the ports of peripheral interface adapter (8255) for input or output. Then the program goes into a software "wait" state and waits for the SBC BASIC-52 to send a "ready" signal.

In the meantime, the SBC BASIC-52 does auto baud rate generation for communication with the monitor it is interfaced with. The user is asked to input the power system parameters viz., the rated voltage and current. The processor calculates the scaling factors for voltage, current and power using these system parameters. Then the processor executes a software routine for formatting the display on the monitor screen, in a tabular format. After displaying this format the SBC BASIC-52 sends a *ready* signal to SBC-8051.

Now both the processors start operating in parallel. The SBC-8051 continually digitizes the input signals at the rate of 8 samples per cycle. It also does its share of computations. The rms values of voltages and currents and active and reactive powers for the three phases are computed every half cycle.

The SBC BASIC-52 simultaneously computes other parameters of the system. It then scales all the parameters to be displayed, and displays them in the table that has been formed on the monitor screen. One complete computational cycle on SBC BASIC-52 including scaling and display takes approximately 0.5 seconds. This means that the data on the monitor screen can be updated every 0.5 sec. For an indicating instrument this is a reasonable rate to update the display.

The results of the computations performed by the SBC-51 are accumulated in the memory for 32 cycles, i.e. approximately 0.5 seconds. After each block of 32 cycles, the SBC-8051 sends an interrupt signal to the SBC BASIC-52 and transfers the accumulated values of computations to SBC BASIC-52. Since one of the restrictions of using BASIC-52 computer is that no interrupts are permitted while a BASIC subroutine is being called from assembly language program, the SBC BASIC-52 waits for the SBC-8051 to transfer data.

The above process continues indefinitely.

5.6 Concluding Remarks

In this chapter, the implementation of the software and the operation of the instrument are described. The software for the SBC-8051 is divided into a number of subroutines, namely, an EORW algorithm subroutine, a 16-bit multiplication subroutine, an active and reactive power subroutine and an rms value computation subroutine. The organization of the data memory is also described in this chapter. The handling of data using on-chip RAM and external RAM is organized in order to reduce the operation time. The concept of paging is used to store the data in the external RAM: all of the data for one phase are stored in one page of memory.

The software for the SBC BASIC-52 is also divided into a number of subroutines which compute, scale and display the various parameters. Lastly, the operation of the instrument, starting from power-up, is described. The test procedures applied to the prototype instrument and their results are presented in the next chapter.

CHAPTER 6
LABORATORY TESTING AND RESULTS

6.1 Introduction

This chapter describes the test procedures applied to the prototype instrument and also the results of those tests. The tests were performed both for steady state and dynamic conditions. These tests were performed primarily to find the accuracy of the instrument for various load and frequency conditions.

The tests to determine the accuracy of voltage, current and power measurements were performed using the configuration illustrated in Figure 6.1. The experimental setup consisted of a function generator, LPA11-K peripheral device and VAX 11/780 computer. The LPA11-K is a microprocessor based peripheral device that consists of analog to digital converters, digital to analog converters and real time clocks. This device is connected to the VAX-11 through the UNIBUS adapter. The device facilitates aggregate analog input and output rates up to 150,000 samples per second with a 12-bit analog to digital converter. The LPA11-K package has a 12-bit analog to digital converter and converts voltage inputs from -5 volts to +5 volts, to the digital numbers from 0 to 4095 respectively. The level 0 volts is represented by the number 2048.

The inputs used in the experiments were simultaneously processed by the instrument and the VAX 11/780 computer. In VAX 11/780 computer the inputs were digitized at the rate of 10,000 samples per second using LPA11-K package. The digitized values were processed on VAX-11/780 computer for calculating the reference values. The parameters of the inputs were determined by VAX-11/780 computer using the maximum and minimum values of the digitized samples. These values are referred to as the "true" values. The parameters displayed on the instrument were compared with the values calculated by the VAX 11/780 computer to determine the accuracy of the measurements.

To generate the input signals, a WAVETEK Model 180 function generator was used. Sinusoidal voltage and current inputs were supplied from the function generator to

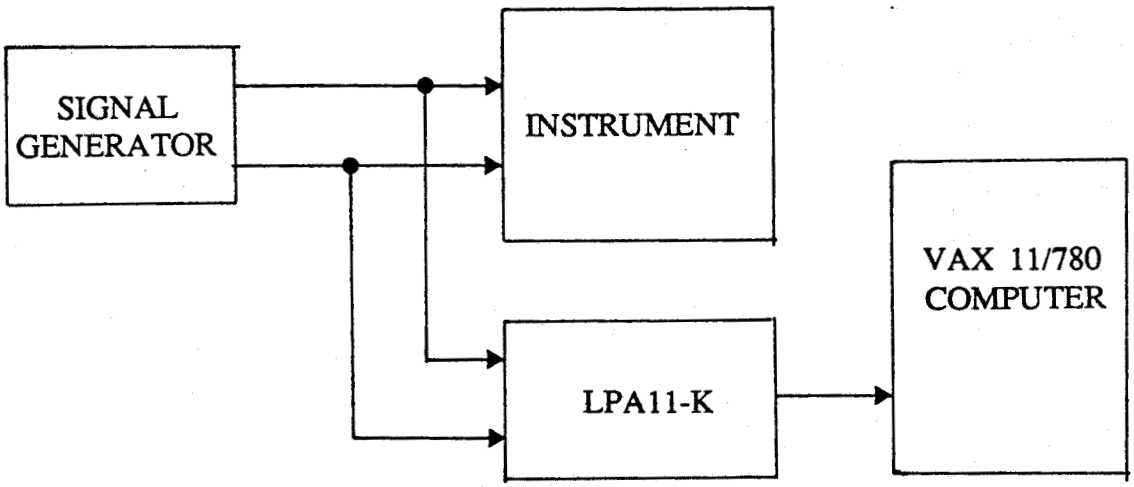

Figure 6.1. Apparatus configuration for performing the tests.

the instrument. This procedure is in order because, in practice, the current signals will be first converted to proportional voltages. To introduce a phase shift between the voltage and current signals, a circuit consisting of a resistor and a capacitor connected in series was used.

A laboratory universal counter, HEWLETT-PACKARD model 5315A, was used in the frequency meter mode for frequency measurements. The universal counter was also used in the timer mode to compute the reference values of the power factor. The time interval between the zero crossings of the input voltage and current waveforms were determined using the counter and the phase angle between them was computed from the time interval.

6.2 Voltage, Current, and Power Measurements

The true rms values of the voltage and current signals were determined from the minimum and maximum values of the digitized samples, S_{min} and S_{max} respectively using Equation 6.1.

$$True\ RMS\ Value = \frac{1}{\sqrt{2}}\left[\frac{(S_{max}-S_{min})\times 10}{4096}\right] \tag{6.1}$$

The true values of the active and reactive powers were determined using the rms values of the voltage and current and the power factor which was determined using the universal counter.

These tests were conducted for loads at three different power factors, that is with resistive loads, capacitive loads and inductive loads. Since the instrument computes the values of the parameters for each phase separately, the tests were conducted on one phase only. For resistive load tests, the voltage input to the instrument was fixed at the rated value and the current input was provided through a 1 kΩ potentiometer. The current input signal was varied from 10% to 150% of the rated value.

Figure 6.2 shows the percentage errors in the measurement of the rms values of the current at various levels of loads. The accuracy of the voltage measurements would be the same as that of the current measurements. The percentage errors in the measurements of the active power for various loads at unity power factor are shown in Figure 6.3. The absolute error in the measurement of the reactive power varied between 0 and 0.002 p.u. during the tests with resistive loads. Ideally, the reactive power should be zero for a resistive load.

The errors in the measurements of the rms values of the voltage and current, and the errors in the measurements of the active power at small loads are observed to exceed 2% in some cases. This is attributed to the increase in the effect of digitization error at small signal levels. It is observed that the errors for all loads more than 25% of the full load are less than 0.5%. It is also found that the errors are always negative, which means that the values computed by the instrument are always less than the actual values.

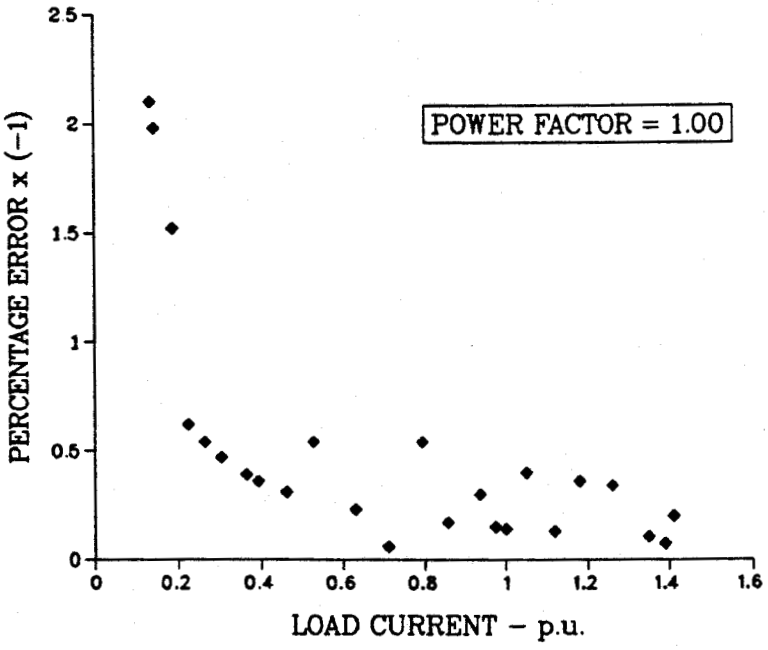

Figure 6.2. Percentage errors in the measurement of current at various loads.

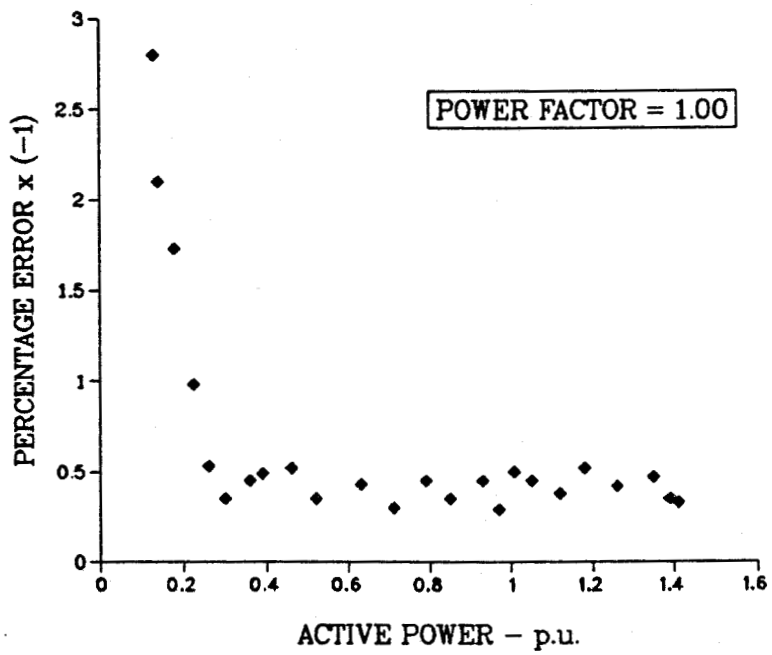

Figure 6.3. Percentage errors in the measurement of active power for resistive loads.

To find the accuracy of the measurements for capacitive loads, an R-C circuit was used to shift the phase of the current signal with respect to the voltage signal. A 0.37 μF capacitor was used in series with a 10 kΩ resistor, as shown in Figure 6.4. The voltage across the resistor represented the current input signal to the instrument. The voltage input to the instrument was connected through a 1 kΩ potentiometer to simulate changes in the active and reactive powers. It may be noted that the amplitude of the current signal input could not be varied using a potentiometer as this would have changed the power factor. Different values of the current signals were obtained by changing the output of the signal generator.

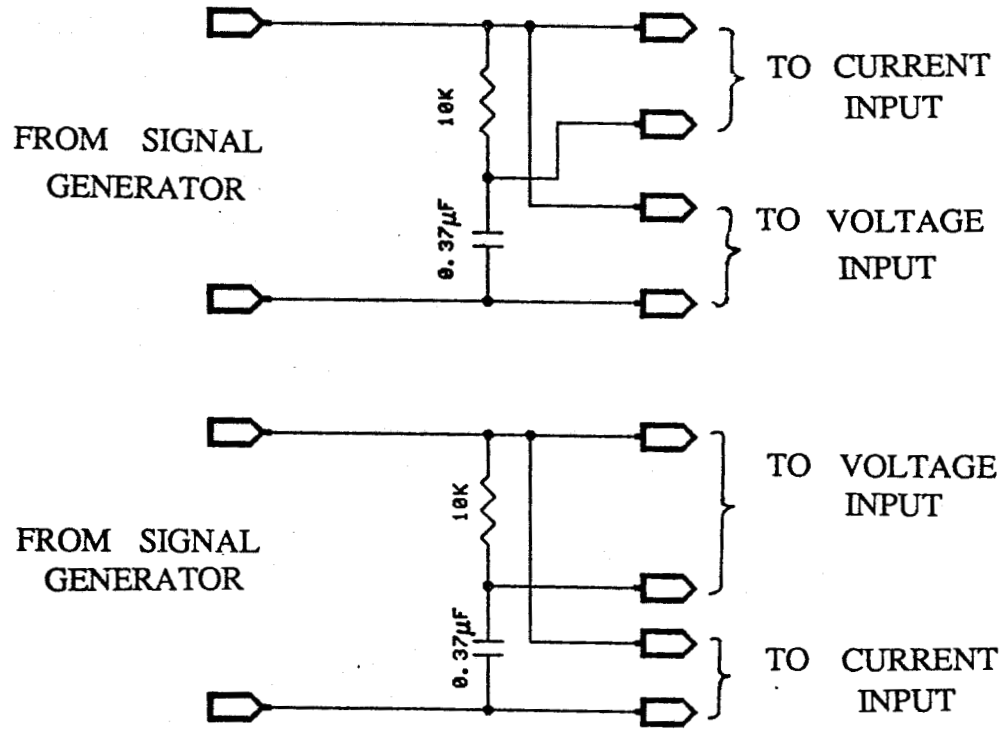

Figure 6.4. Circuit for simulating capacitive and inductive loads.

The percentage errors in the measurements of active and reactive powers for various loads at 0.8 leading power factor are shown in Figures 6.5 and 6.6 respectively. Similar to the case of the resistive loads, the errors in the measurements at small loads are found to exceed 2.5% in some cases. However, the errors for all loads more than 25% of the full load are less than 0.7%. The errors in the measurements of the reactive power are

found to be positive because the reactive power for capacitive loads is negative.

The R-C circuit used for capacitive load tests was also used to conduct tests for inductive loads. In this case the output of the R-C circuit was connected to the voltage input of the instrument. The output of the function generator was connected through a potentiometer to the current input of the instrument. Since the phase of the voltage signal leads the current signal, the arrangement simulated inductive loads. The percentage errors in the measurements of active and reactive powers are shown in Figures 6.7 and 6.8 respectively. The accuracy of the measurements is found to be similar to that for the case of capacitive loads. The errors are always found to be negative.

6.3 Effect of Frequency Compensation

This test was conducted to determine the error in the measurements due to variations in the input signal frequency. For this test the frequency compensation section was excluded from the program and the sampling rate was fixed at 480 samples per second. The accuracy of the measurements of the load current was determined for various frequencies between 55 and 65 Hz. Figure 6.9 shows the percentage errors in the measurement of the rms values of load current (near rated value), as the frequency was varied. It is found that the errors are negative when the frequency is less than the nominal value (60 Hz in this case) and are positive when the frequency is more than the nominal value. The error increases as the frequency deviation from the nominal frequency increases.

A similar test was performed with the automatic frequency compensation included, i.e., the sampling rate was controlled to 8 samples per cycle regardless of the signal frequency. The frequency was varied between 55 and 65 Hz. No change in the values of the parameters was observed as the frequency was varied. Over the selected range of frequency, the output amplitude of the function generator was constant.

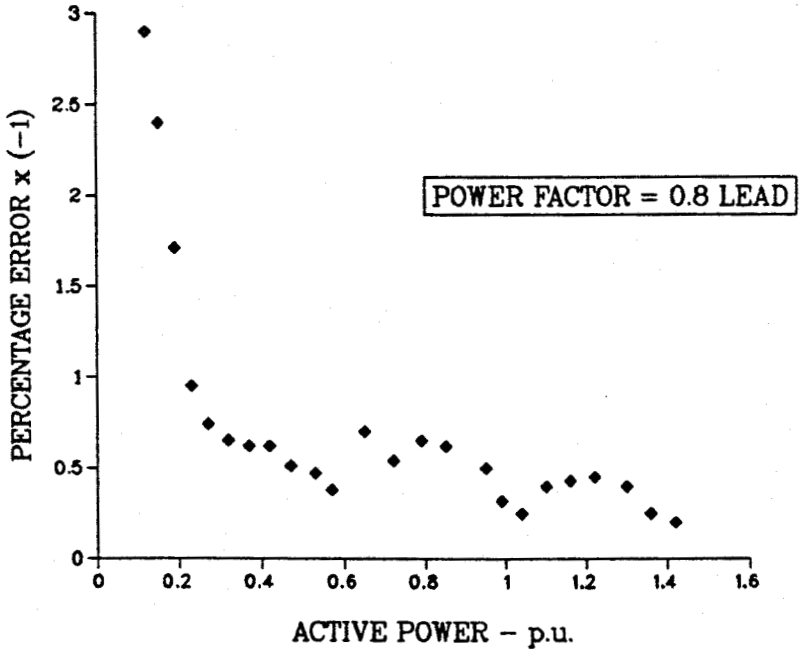

Figure 6.5. Percentage errors in the measurement of active power for capacitive loads.

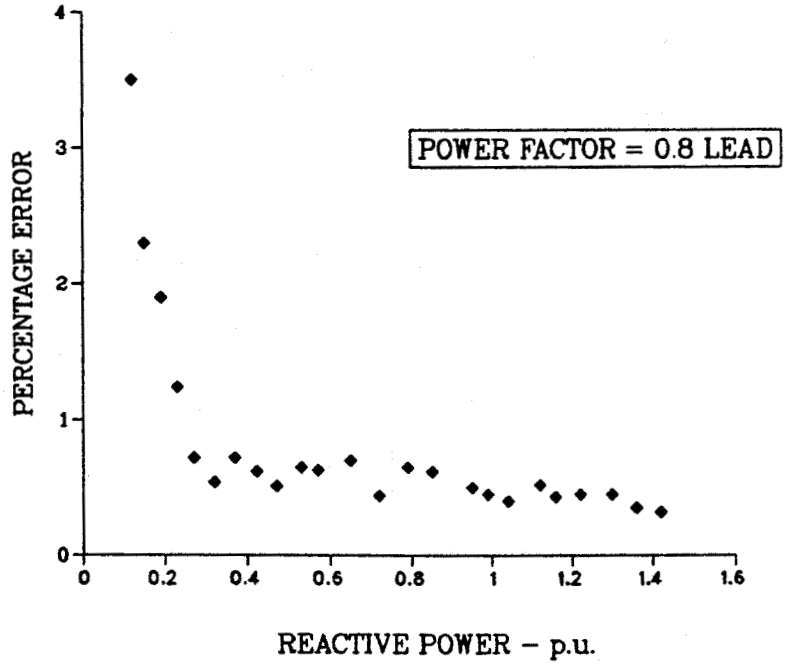

Figure 6.6. Percentage errors in the measurement of reactive power for capacitive loads.

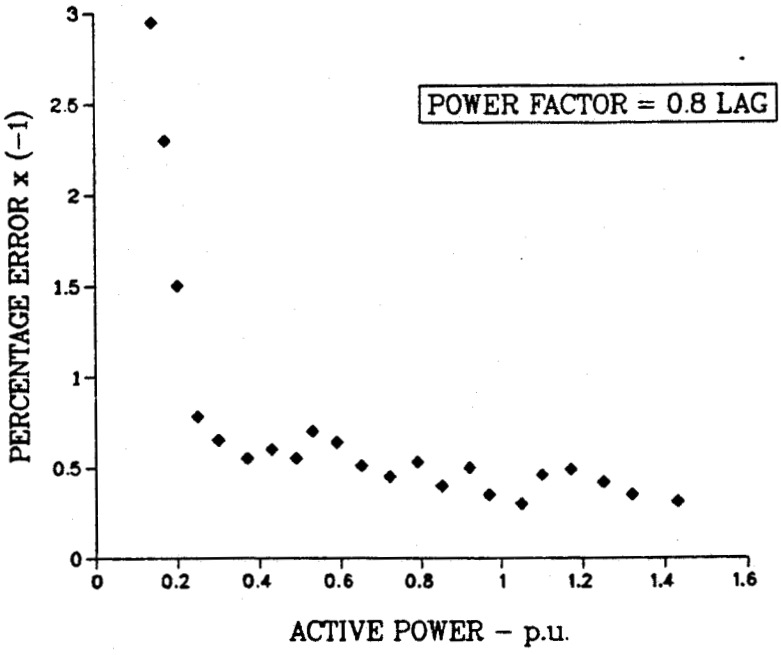

Figure 6.7. Percentage errors in the measurement of active power for inductive loads.

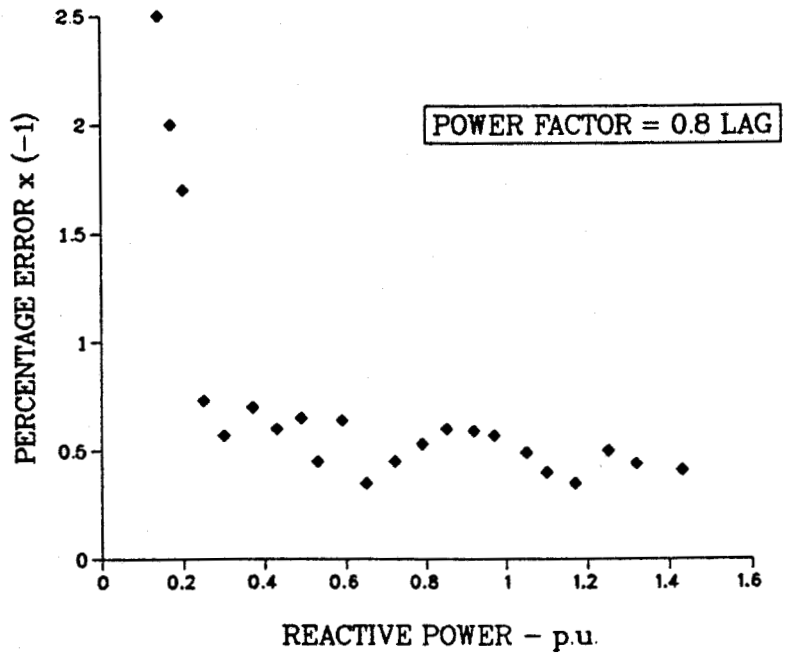

Figure 6.8. Percentage errors in the measurement of reactive power for inductive loads.

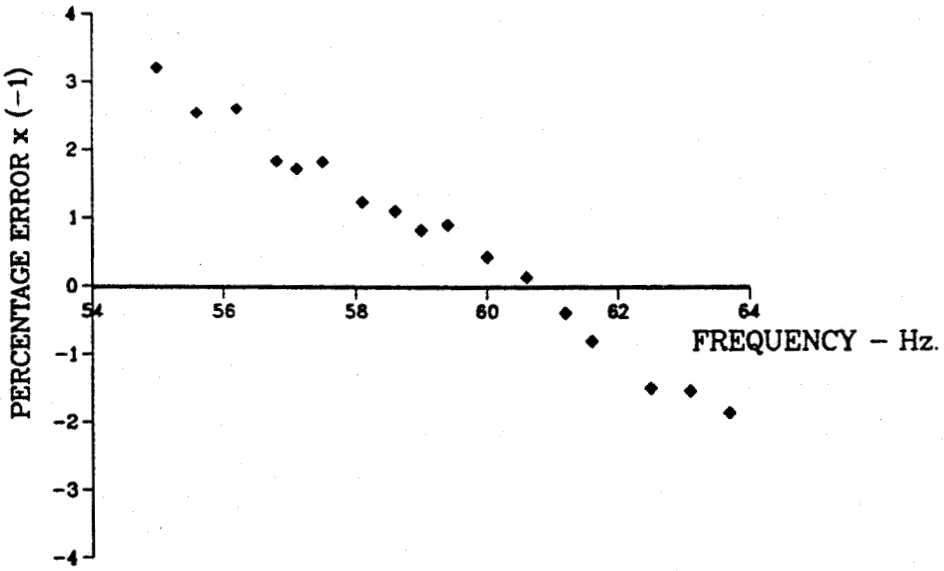

Figure 6.9. Percentage errors in the measurement of current as a function of frequency, if the frequency compensation is not applied.

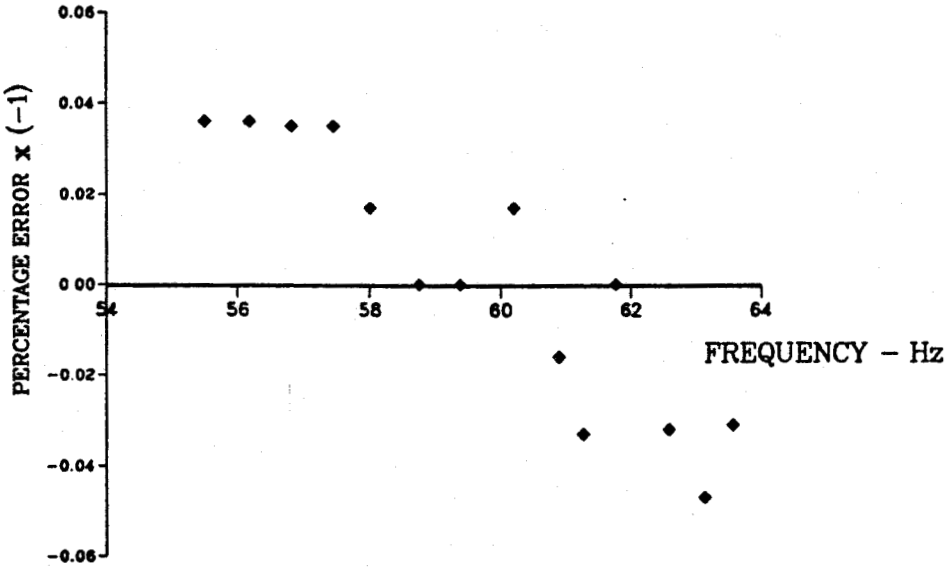

Figure 6.10. Percentage errors in the measurement of frequency.

6.4 Frequency Measurement

The errors in the measurements of frequency were determined using a standard laboratory frequency meter as reference. The frequency of the signal from the signal generator, at a constant amplitude, was varied from 55 Hz to 65 Hz. The percentage error in the measurement of the frequency was found to be less than 0.04%. The results are illustrated in the Figure 6.10.

6.5 Power Factor Measurement

The errors in the measurements of the power factor were determined by comparing the values calculated by the instrument with the values obtained using the universal counter. The test was conducted for power factors from 0.5 lagging to 1.0 and from 0.5 leading to 1.0. The capacitive and inductive load effects were simulated in the manner explained in section 6.2. The results are illustrated in Figure 6.11. This figure shows that the absolute errors are less than 0.02. The errors in the measurement of power factor for values below 0.5 are higher, from 0.03 to 0.04 in some cases.

6.6 Energy Measurement

The errors in the measurements of energy were determined using the calculated powers for a selected time. The powers were kept constant for a selected time and then the values of kWh and kVArh were determined using the time and the powers. It was found that the errors in the measurements of energy were of the same order as the errors observed in the measurements of powers. This is attributed to the fact that the energy is being determined by integrating power over time and the system uses a timer that is run by an accurate crystal oscillator.

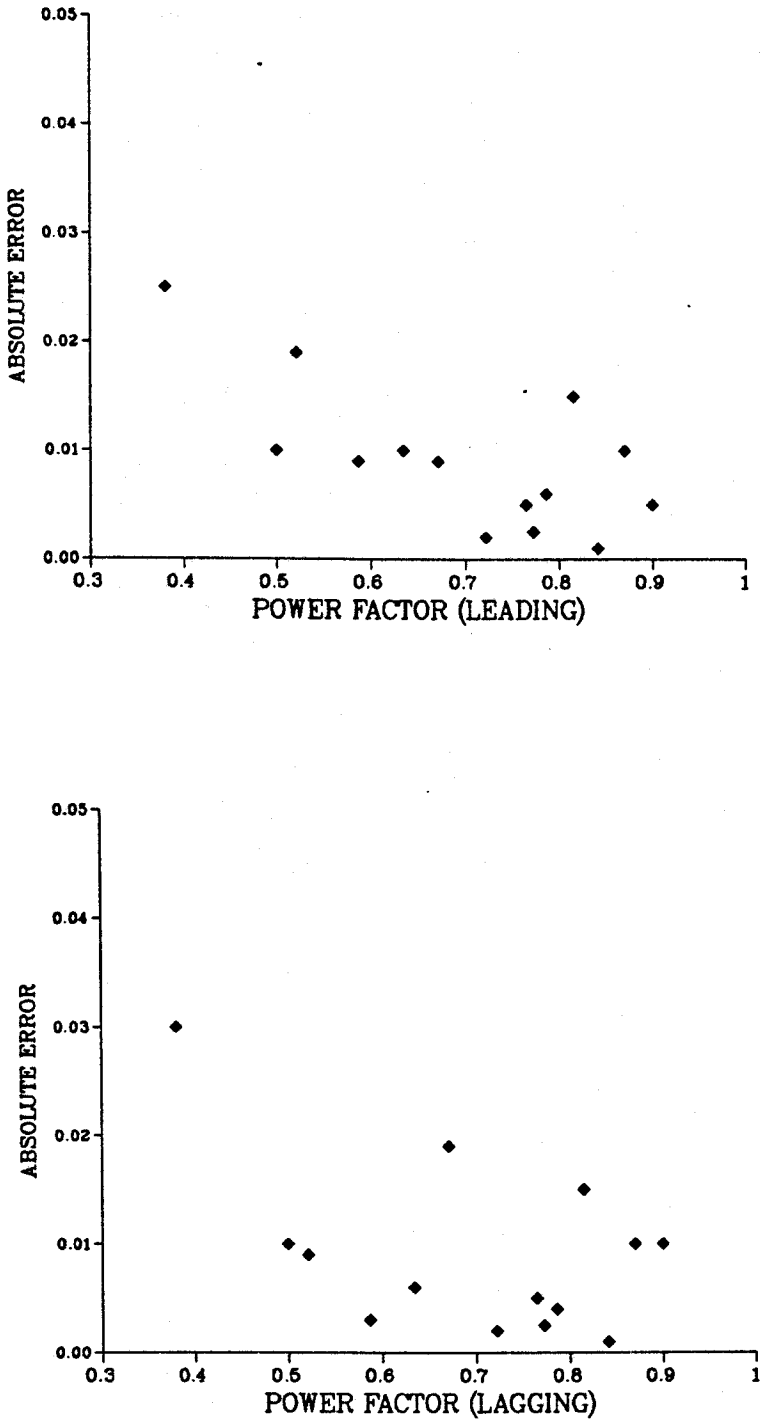

Figure 6.11. Percentage errors in the measurement of power factor.

6.7 Dynamic Tests

The dynamic tests were conducted for determining the response of the instrument to sudden changes in the inputs. To conduct the tests, the inputs were varied and the time taken by the instrument to display a stable value was noted. As explained earlier, the display on the monitor screen is updated every half second. It was observed during these tests that for any change in the amplitude of the input signals it takes a maximum of 2 to 3 cycles of the display update (1 to 1.5 seconds) to attain the steady state values. It was also observed that for any change in the frequency, it takes two cycles of the display update for the displayed frequency value to stabilize. It can be concluded from the tests that it takes 1 to 1.5 seconds for the output to stabilize after a change in the inputs is experienced.

6.8 Concluding Remarks

The test procedures applied to the prototype instrument, and their results, were discussed in this chapter. These tests were performed to measure the accuracy of the instrument under various operating conditions. The Laboratory Peripheral Accelerator on a VAX-11/780 computer was used to determine the reference values for most of the tests conducted on the instrument. The inputs were processed simultaneously on the VAX-11/780 and the instrument and the results were compared. The accuracies of the instrument are found to be well within the limits specified in the specifications.

CHAPTER 7

CONCLUSIONS

The objectives of this study were to design, fabricate, and test a prototype multi-function microprocessor-based instrument to measure, and display in real time, parameters of a 3-phase power system, such as currents, voltages, active and reactive powers, energies, power factors and frequency.

A number of algorithms suitable for determining the phasor components of a sinusoidal waveform were studied to identify their strengths and weaknesses. An algorithm based on the correlation of a sinusoidal function to a pair of orthogonal functions was chosen for use in the instrument. This algorithm is called the EORW algorithm. The advantages of using this algorithm are that its evaluation involves simple additions and subtractions which are easy to implement on an inexpensive microprocessor. The algorithm also attenuates some harmonics that might be present in the input signal.

Using the phasor components of the voltage and current signals, the voltages, currents, active and reactive powers, energies (kWh & kVArh), and power factors in a 3-phase power system are computed. A numerical technique, called the Piecewise Linear Approximation, has been used to evaluate the rms values of voltages and currents from their real and imaginary components.

The frequency is measured using a phase-locked-loop (PLL) technique. A frequency multiplier circuit using a PLL multiplies the frequency of the input voltage. A stable crystal oscillator is used as a frequency reference. This circuit is also used to control the sampling rate so that exactly eight samples are taken in each power frequency cycle irrespective of the frequency of the input signal. This avoids errors in the outputs due to drift in the frequency of the input signals.

The power system parameters for all three phases are computed and displayed in real time. For the computations and for performing the control functions of the instrument two single-board microcomputers have been used. These microcomputers are based on the INTEL 8051 and 8052 microcontrollers and operate in parallel. The use of

two single board microcomputers has increased the computational speed. Other hardware for the system consists of analog filters, a digitization unit, a frequency multiplier circuit and a display unit.

Switched capacitor type 6th order Butterworth filters, in low pass configuration, have been used to attenuate the non-fundamental components of the input voltages and currents. The digitization unit consists of a 12-bit analog to digital converter, sample and hold circuits, and multiplexers. A video terminal displays the output of the instrument. All hardware circuits have been constructed as printed circuit boards or as wire-wrapped modules, and have been installed in a cabinet.

Several experiments were performed in the laboratory to simulate load conditions to test the instrument. For resistive loads, steady state errors of less than 0.5% of the full scale were observed in the measured rms voltages, currents, and active and reactive powers. For combinations of resistive and reactive loads, which represent the actual loading conditions in a power system, the errors were less than 0.7% of the full scale. For frequency measurements, the maximum errors observed were less than 0.04%. The maximum error in the measured power factors was observed to be 0.03. Since the time can be measured very accurately by using a crystal oscillator, the accuracy of the energy measurements was found to be of the same order as the accuracy of the power measurements.

This project has demonstrated that an instrument that has acceptable accuracy and is versatile can be designed using inexpensive microcontrollers. The developed instrument is for a metering application. However, the same instrument, with some software and hardware modifications could also act as a transducer to provide signals for control applications in a power system. The usefulness of such a transducer would have to be studied further considering factors such as response time and accuracy. The results presented in Chapter 6 indicate that the error in the measurement of the parameters are always positive and are predictable. Therefore, the accuracy of the instrument could be improved further by including an appropriate offset compensation in the instrument.

With small changes in the software, other features such as power demand at any time and maximum demand in a given period could be included. Features, such as precautionary alarm to alert an operator when a selected parameter exceeds a threshold could also be included in the instrument. The instrument could also send the system parameter data to a data logging unit at the sub-station. In case of a power failure, the energy measurements must be saved. To facilitate this, a mechanical counter could be connected to the instrument to keep a record of the energy values.

In practice, this instrument would replace several instruments from the control panel or desk in a power generating station or a sub-station. This would result in a more compact control desk which would mean that the operator would no longer be required to scan a number of separate instruments. The information is provided to the operator in a concise and compact form, and can be automatically stored for subsequent analysis and permanent record.

REFERENCES

[1] Handscombe, E., *Electrical Measuring Instruments,* The Wykeham Technological Series, Wykeham Publications Ltd., London.

[2] The New Encyclopedia Britainnica, Knowledge in Depth, *Instrumentation,* page 631-632, 15th edition, 1984.

[3] Modern Power System Practice vol. 6, *"Instrumentation Controls and Testing",* Pergamon Pres, 1972.

[4] Golding, E.W. and Widdis, F.C., *"Electrical Measurements and Measuring Instruments"* Sir Issac Pitman & Sons Ltd., 1963.

[5] The Solid State Meter - a user's viewpoint, 2nd International conference on *Metering, Apparatus and Tariffs for Electricity,* organized by Power Division of IEE.

[6] Makino, J. and Miki, Y., "Study of Operating Principles and Digital Filters for Protective Relays with Digital Computer", IEEE PES Winter Power Meeting, New York, 1975, Paper No. C75 197-9.

[7] Mann, B. J. and Morrison, I. F., "Digital Calculation of Impedances for Transmission Line Protection", *IEEE Transactions on Power Apparatus and Systems,* Vol. PAS-90, No. 1, Jan./Feb. 1971, pp. 270-279.

[8] Gilcrest, G. B., Rockefeller, G. D. and Udren, E. A., "High Speed Distance Relaying Using a Digital Computer Part-I-System Description", *IEEE Transactions on Power Apparatus and Systems,* Vol. PAS-91, No. 3, May/June 1972, pp.1235-1243.

[9] Rockefeller, G. D. and Udren, E. A., "High Speed Distance Relaying Using a Digital Computer Part-II", *IEEE Transactions on Power Apparatus and Systems,* Vol. PAS-91, No. 3, May/June 1972, pp.1244-1256.

[10] Sachdev, M. S. and Wood, H. C., "Introduction and General Methodology of Digital Protection", Canadian Electrical Association Spring Meeting - March 1986, Toronto.

[11] Ramamoorty, M., "A Note on Impedance Measurement Using Digital Computer", *IEE-IRE Proceeding (India)* Vol. 9, No. 6, Nov./Dec. 1974, pp. 243-247.

[12] Phadke, A. G., Hlibka, T. and Ibrahim, M., "A Digital Computer System for EHV Substations: Analysis and Field Tests", *IEEE Transactions on Power Apparatus and Systems,* Vol. PAS-95, No. 1, Jan./Feb. 1976, pp. 291-301.

[13] Hope, G. S. and Umamaheswaran V. S., "Sampling for Computer Protection of Transmission Lines", *IEEE Transactions on Power and Apparatus and Systems,* Vol. PAS-93, No. 5, Sept./Oct. 1974, pp. 1522-1533.

[14] Luckett, R. G., Munday, P. J. and Murray, B. E., "A Substation Based Computer for Control and Protection", IEE Conference Publication No. 125, London, March, 1975, pp.252-260.

[15] Brooks, A. E., "Distance Relaying Using Least Squares Estimates of Voltage, Current and Impedance", Proceeding of 10th Power Industry Computer Application Conference, May, 1977, pp. 394-402.

[16] Sachdev, M. S., and Baribeau, M. A., "A New Algorithm for Digital Impedance Relays", *IEEE Transactions on Power and Apparatus and Systems*, Vol. PAS-98, No. 6, Nov./Dec. 1979, pp. 2232-2240.

[17] Schweitzer, E. O. and Aliaga Antenor, "Digital Programmable Time-Parameter Relay offers Versatility and Accuracy", *IEEE Transactions on Power Apparatus and Systems*, Vol. PAS-99, No. 1, Jan./Feb. 1980.

[18] Sachdev, M. S., Coordinator, "Computer Relaying, Tutorial Text", Publication No. 79 EH 0148-7-PWR, IEEE, New York, 1979.

[19] American National Standard C39.1-1981, *Requirements for Electrical Analog Indicating Instruments*, published by American National Standards Institute, Inc.

[20] IEEE Standard 120-1955, *measurement* published by American Institute of Electrical Engineers.

[21] IEEE Standard. 108-1955, *Proposed Recommended Guide for Specification of Electronic Voltmeters*, published by American Institute of Electrical Engineers.

[22] Sidhu T. S., *Computer-Aided Design and Performance Evaluation of Digital Relays*, M.Sc. Thesis, August 1985, University of Saskatchewan, Saskatoon.

[23] *INTELLEC SERIES IV OPERATING AND PROGRAMMING GUIDE, 1984* published by Intel Corporation.

[24] The ICE-51, *In-Circuit Emulation System - 51 Guide*, published by Intel Corporation.

[25] *Microcontroller Handbook 1984* Intel Corporation, Order No. 210918.

[26] The iAPX-86 Book, *published by Intel Corporation.*

[27] *Switched Capacitor Filter Handbook 1985*, National Semiconductor Corporation.

[28] *Intersil Databook - 1981*, Intersil Inc., California.

[29] *CMOS Integrated Circuits Databook 1976-77*, Solid State Scientific Inc.

[30] *Analog and Telecommunications Product Databook 1984*, Volume 4, Harris Corporation.

[31] *Linear Databook 1978*, National Semiconductor Corporation.

[32] Allen Systems FX-31, 1984, Columbus, Ohio.

[33] The Micromint Inc. BCC-52, 1985, Vermon, Connecticut.

[34] Qume Corporation, QVT 101 Operator Manual, Jan. 1985.

[35] *Data-Acquisition Databook 1982*, Volume 1, Integrated Circuits, Analog Devices.

[36] Oppenheim, A. V. and Schafer R. W., *Digital Signal Processing*, Prentice Hall Inc., Englewood Cliffs, N.J., 1978.

APPENDIX - A

8051/8052 Architecture and Memory Organization

A.1 General

The Intel 8051/8052 is an 8-bit microcontroller based on HMOS II technology. The architecture is illustrated in Figure A.1 [25]. It has an 8-bit CPU and supports a 16-bit external address and 8-bit external data bus. The lower 8-bits of the address lines are multiplexed to form the data bus. If no external memory is used, the processor can support 32 Input-Output lines. The processor has three separate memory spaces - a 64 K-byte program memory space, a 64 K-byte external data memory space, and a 128 (256)* byte internal RAM space. It has a five (six)* source interrupt structure with two priority levels. Two (three)* 16-bit hardware timers/counters and one asynchronous serial port (UART) are also provided on the processor. An on-chip oscillator with clock circuitry is also present in this 40-pin package. It uses TTL compatible memories and most byte oriented peripherals for additional I/O and memory capabilities.

The 8051 microcontroller makes efficient use of its program memory space with an instruction set consisting of 44% one-byte, 41% two-bye and 15% three byte instructions. At 12 MHz clock rate more than 50% instructions execute in 1.0 μsec. The Pin Configuration of both 8051 and 8052 microcontrollers is shown in the Figure A.2.

A.2 Memory Organization

The 8051 has separate address spaces for Program Memory and Data Memory. The Program memory can be upto 64K bytes long. The lower 4K (8K for 8052) bytes may reside on-chip. The data memory can consist of up to 64K bytes of off-chip RAM and in addition includes 128 bytes of on-chip RAM (256 bytes for the 8052) plus a number of Special Function Registers "SFRs", some of which are listed below:

---

* For 8052 processor only.

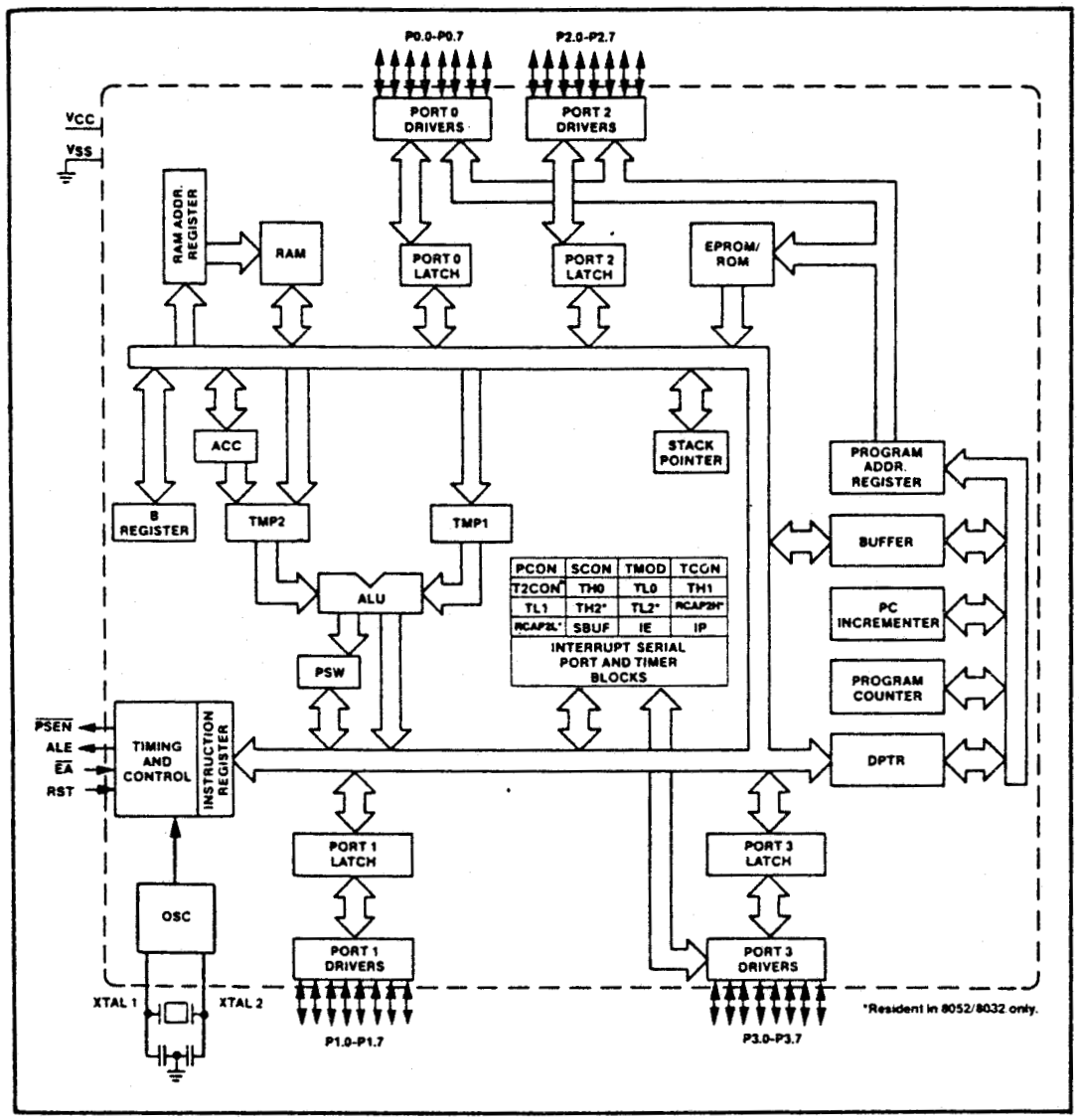

Figure A.1. Architecture of 8051/8052 Microcontrollers.

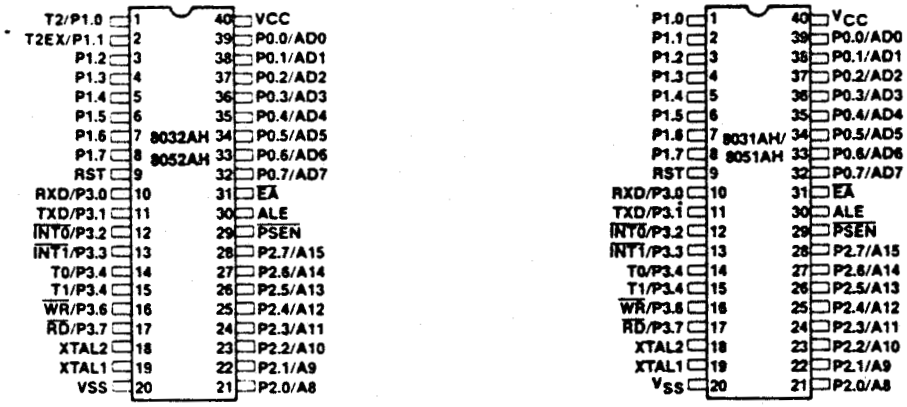

Figure A.2. Pin Configuration of 8051 & 8052 Microcontrollers.

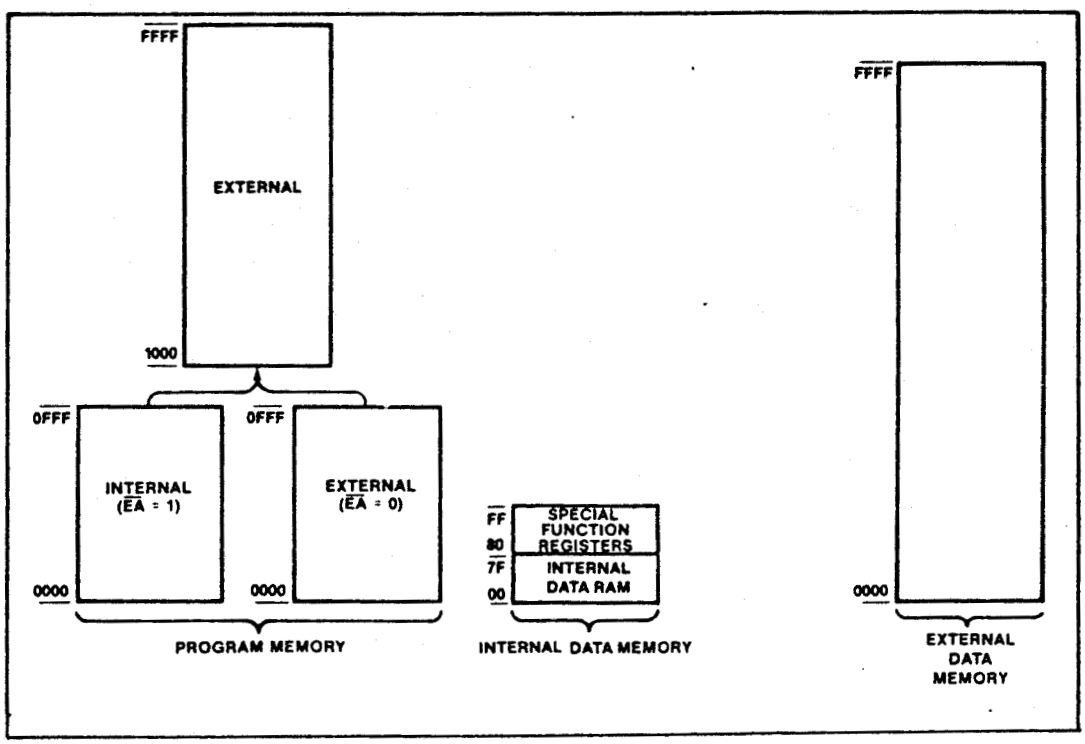

Figure A.3. Memory Maps for Microcontroller-51.

Symbol	Name	Address†
ACC*	Accumulator	0E0H
B*	B Register	0F0H
PSW*	Program Status Word	0D0H
SP	Stack Pointer	81H
DPTR	Data Pointer (consist-	83H
	ing of DPH and DPL)	82H
P0*	Port 0	80H
P1*	Port 1	90H
P2*	Port 2	0A0H
P3*	Port 3	0B0H
IP*	Interrupt Priority Control	0B8H
IE*	Interrupt Enable Control	0A8H
TMOD	Timer/Counter Mode Control	89H
TCON	Timer/Counter 2 Control	0C8H
TH0	Timer/Counter 0 high byte	8CH
TL0	Timer/Counter 0 low byte	8AH
TH1	Timer/Counter 1 high byte	8DH
TL1	Timer/Counter 1 low byte	8BH

The SFRs marked with an asterisk (*) are both bit- and byte- addressable. Figure A.3 shows microcontroller-51 memory maps.

† Addresses are given in hexa-decimal numbers.

A.2.1 Program Memory Address Space

The 64K-byte Program Memory consists of an internal and an external memory portion. If the $\overline{EA}$ pin is held high, the 8051 executes out of internal program memory unless the address exceeds 0FFFH (1FFFH for 8052). Locations 1000H through 0FFFFH (2000H through 0FFFFH for the 8052), are then fetched from external Program memory. If the $\overline{EA}$ pin is held low, the 8051 fetches all instructions from external Program Memory. In either case the 16-bit program counter is the addressing mechanism.

Locations 00 through 23H (00 through 2BH for the 8052) in the Program Memory are used by interrupt service routines as indicated in Table A.1.

A.2.2 Data Memory Address Space

The Data Memory address space consists of an internal and an external memory space. External Data Memory is accessed when a MOVX instruction is executed.

Internal Data Memory is divided into two (three in 8052) physically separate and distinct blocks: the lower 128 bytes of RAM, the upper 128 bytes of RAM (accessible in the 8052 only) and 128-byte Special Function Register (SFR) area. Figure A.4 shows a mapping of Internal Data Memory. Four 8-Register Banks occupy locations 0 through 31 in the lower RAM area. Only one of these banks may be enabled at a time (through a 2-bit field in PSW). The next sixteen bytes comprising of locations 32 through 47 contain 128 bit addressable locations.

A.3 Addressing Modes

The 8051 uses five addressing modes viz. :

- Register
- Direct
- Register Indirect

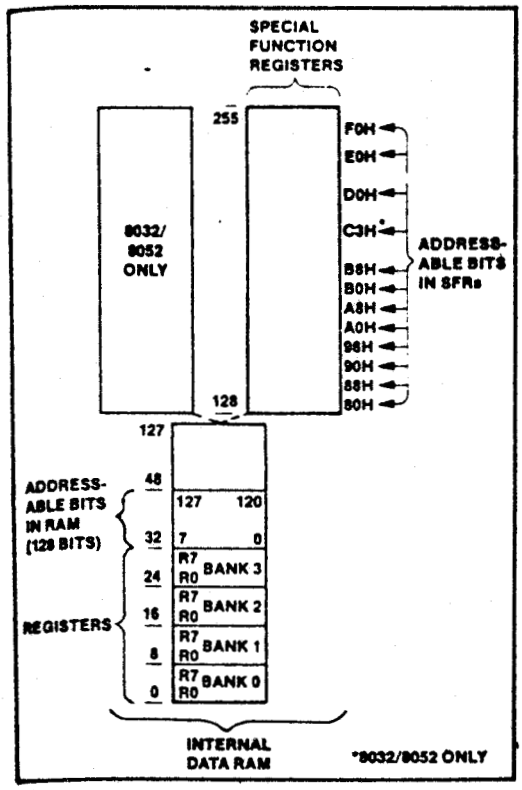

Figure A.4. Mapping of Internal Data Memory.

Table A.1 : Interrupt Vector Locations.

Source	Address
External Interrupt 0	0003H
Timer 0 Overflow	000BH
External Interrupt 1	0013H
Timer 1 Overflow	001BH
Serial Port	0023H
Timer 2 Overflow	002BH

- Immediate
- Base-Register plus Index-Register Indirect.

Table A.2 summarizes the memory spaces that have access through each of the addressing modes.

A.3.1 Register Addressing

Register addressing accesses the eight working registers (R0 - R7) of the selected Register Bank. The least significant three bits of the instruction op code indicate the register to be used. ACC, B, DPTR and CY can also be addressed as registers.

A.3.2 Direct Addressing

Direct addressing is the only method of accessing the Special Function Registers. The lower 128 bytes of Internal RAM can also be directly addressed.

Table A.2 : Addressing Method and Associated Memory Spaces.

Register Addressing
– R0 - R7
– ACC, B, CY(bit), DPTR
Direct Addressing
– Lower 128 bytes of internal RAM
– Special Function Registers
Register Indirect Addressing
– Internal RAM (@R1, @R0, SP)
– External Data Memory (@R1, @R0, @DPTR)
Immediate Addressing
– Program Memory
Base + Index Indirect Addressing
– Program Memory (@DPTR + A, @PC + A)

A.3.3 Register-Indirect Addressing

Register-Indirect Addressing uses the contents of either R0 or R1 (in the selected Register Bank) as a pointer to locations in a 256-byte block: the lower 128-bytes of internal RAM, the upper 128-bytes of internal RAM (8052 only) or the lower 256 bytes of external Data Memory. However, the Special Function Registers are not accessible by this method. Access to the full 64K external Data Memory address space is accomplished by using the 16-bit Data Pointer.

A.3.4 Immediate Addressing

Immediate Addressing allows constants to be part of the op code instruction in Program Memory.

A.3.5 Base-Register Plus Index Register-Indirect Addressing

Base-Register plus Index Register-Indirect Addressing allows a byte to be accessed from Program Memory via an indirect move from the location whose address is the sum of a base register, DPTR or PC and an index register, ACC. This mode facilitates look-up-table accesses.

APPENDIX - B

SINGLE BOARD MICRO-COMPUTERS FX-31 AND BCC-52

B.1 SBC FX-31

Allen System's FX-31 Computer Board [32] is a general purpose single board computer utilizing Intel's 8031 microcontroller (ROMless version of Intel's 8051). Most of the board's capabilities result directly from the 8031. This 40-pin DIP IC consists of a full duplex UART, two 16-bit timer/counters, a Boolean processor, two 8-bit parallel ports and 128 bytes of internal data RAM. It is obvious that a large number of resources are available on the 8031 for control oriented applications.

A standard 6.5 inch long by 4.5 inch wide board size is used to incorporate the design. A 22/44 pin standard finger connector allows the necessary lines to be brought out over a 44 line connector bus (non-standard). Additionally, a 40 pin connector is employed at one end to provide access to the board's four parallel ports, TTL serial lines, and RS-232C serial lines.

The general memory setup allows for 4 memory IC's to be interfaced with the processor. Two of these memory IC's are dedicated to the 8031's code space, that is these devices must be EPROM devices containing processor instructions. The other two memory IC's are configurable to either EPROMs or RAMs via board jumpering.

The board's memory and I/O decoding is performed by a 74LS154 decoder. This IC performs a 4 line to 16 line decoding of address lines A11, A12, A13, and A14. Therefore there are 16 selections of each 2K boundary starting from the address location 0000H. With minor modifications in the board's circuitry (by jumpering) these boundaries can be changed to 4K, 8K or 16K, as desired.

In the minimum configuration, TTL levels of serial transmit and receive lines are available at the 22/44 pin connector as well as the 40 pin I/O connector. In order to convert these lines to RS-232C compatible levels, the board has provisions for installation of 1488 and 1489 buffer IC's. The RS-232C lines are also brought out on the 40 pin I/O connector.

In the minimum configuration , port 1 of 8031 is available for 8-bit parallel input and output at 40 pin connector. Note that each of the port 1 lines can be individually programmed as an input or an output. To expand the number of parallel lines available on the board, a 8255 PIA has been used to provide three additional 8-bit parallel ports. These three ports are all brought out on the 40 pin I/O connector. The chip select to the 8255 is hard-wired on the board. The address which selects the 8255 is a function of the boundary size selected by the user.

B.2 SBC BCC-52

The BCC-52 computer/controller board [33] is based on the Intel's 8052AH-BASIC chip which is a preprogrammed version of the 8052AH microcontroller. The architecture of this chip is discussed in Appendix A. The 8052AH-BASIC has a 16-bit address and an 8-bit data bus. When the chip is powered up it sizes consecutive external memory from 0000H to the end of the memory (or memory failure) by alternatively writing 55H and 00H into each location. A minimum of 1K bytes of RAM is required for BCC-52 to function and the RAM locations must begin at 0000H.

BCC-52 reserves the first 512 bytes of External Data Memory for implementing two "software" stacks: the control stack and the arithmetic stack or Argument Stack. The control stack occupies locations 96 (60H) through 254 (0FEH) in external RAM memory. This memory is used to store all information associated with loop control (i.e. DO-WHILE, DO-UNTIL, and FOR-NEXT) and basic sub-routines (GOSUB). The stack is initialized to 254 (0FEH) and "grows down".

The argument stack occupies locations 301 (12DH) through 510 (1FEH) in external RAM memory. This stack stores all the constants used by BASIC during a program. Operations such as Add, Subtract, Multiply and Divide always operate on the first two numbers on the Argument Stack and return the result to the Argument Stack. The Argument Stack is initialized to 510 (1FEH) and "grows down" as more values are placed on it. Each floating point number placed on the Argument Stack requires 6 BYTES of storage.

There are five main sections of the BCC-52 board : processor, address decoding and memory, parallel I/O, serial I/O, and EPROM programmer.

B.2.1 Address Decoding

The 8052 uses most of the first 32K (0H-7FFFH) as split memory. DATA (RAM) is enabled by the 8052 RD line and PROGRAM memory (EPROM) is enabled by 8052 PSEN line. The three most significant lines (A13-A15) are connected to a 74LS138 decoder chip which separates the addressable range into eight 8K memory segments, each with its own chip select. A second 74LS138 decoder partitions either C800H-CFFFH or E800H-EFFFH as eight 256 byte I/O blocks. This is done to allow multiple peripherals to share the same 256 bytes address range.

B.2.2 Parallel I/O

The BCC-52 contains an 8355 PIA which provides three 8-bit input/output software configurable parallel ports. The three I/O ports labelled A, B, and C and a write only mode configuration register occupy 4 consecutive addresses in one of the 8 jumper selectable I/O blocks. The three parallel ports and the ground are connected to a, 26-pin, flat ribbon cable connector. The outputs are TTL compatible.

B.2.3 Serial I/O

There are two serial ports on BCC-52 board. One is for console I/O terminal and the other is an auxiliary serial output referred to as the line printer port. When using an 11.0592 MHz crystal, the console port does auto baud rate determination on power up (a preset baudrate can be alternatively be stored in EPROM as well). It will function at 19200 bps with no degradation in operation.

The main purpose of the software line printer is to let the user make a "hard copy" of the program listings and/or data. The command LIST# and the statement PRINT# direct outputs to the software line printer port. The maximum baudrate that can be assigned in this case (for communication) is 4800 bps.

MC1488 and 1489 level shifters convert the TTL logic levels from the console and line printer to RS-232C. The BCC-52 requires only about 200 milliamps at +5V to function. ± 12V is required for external RS-232 communication and +21V for the EPROM programming.

B.2.4 EPROM Programmer

One of the powerful feature of the BCC-52 is that it has the ability to execute and save programs in an EPROM. The 8052AH chip generates all the timing signals needed to program 2764/27128 EPROMs. Saving programs in EPROMs is a much more attractive and reliable alternative to cassette tapes, especially in control and/or noisy environments.

BCC-52 does not save a single program on an EPROM (unless the size of the program and the EPROM are the same). In fact, it can save as many programs as the size of EPROM memory permits. The programs are stored sequentially in the EPROM and any program can be retrieved and executed. This sequential storing of programs is referred to as the EPROM FILE.

APPENDIX - C

PEAK VALUE ESTIMATION

C.1 Mathematical Background

The peak values of signals from their real and imaginary components can be computed using Equation C.1.

$$P = \sqrt{(RE^2 + IM^2)} \tag{C.1}$$

If this equation is computed using exact methods, the computation time requirements are high. However, these calculations can be replaced by a Piecewise Linear Approximation technique. Consider that R and I are the real and imaginary parts, respectively of a phasor. Let a and b be defined as follows:

$$a = MAX\ (|R|, |I|), \tag{C.2}$$

$$b = MIN\ (|R|, |I|). \tag{C.3}$$

By selecting the largest and the smallest of R and I, the coefficients or multipliers called x and y can be found in such a way that the peak value p is given by Equation C.4.

$$p = x \,.\, a + y \,.\, b \tag{C.4}$$

This is the case when only one approximation region is considered. However, the number of regions can be more than one and in general for n regions there will be a set of values of x and y such as, (x_1, y_1), (x_2, y_2), ..., (x_n, y_n). Each set of coefficients x and y is valid for a particular range of b/a ratios. The value for each set of coefficients can be calculated using the least error square fit of the data (of a particular region for which the values of x and y are being evaluated) to a linear equation of the form of Equation C.4. If

m is the number of data points used to fit the data from any region (say *nth* region) then in the matrix form it can be written as follows :

$$[p] = [x_n][a] + [y_n][b] \tag{C.5}$$

Values of unknown x_n and y_n can be calculated using Equation C.6.

$$\begin{bmatrix} x_n \\ y_n \end{bmatrix} = \begin{bmatrix} [[a]^T[a]]^{-1}[a]^T[p] \\ [[a]^T[a]]^{-1}[a]^T[p] \end{bmatrix} \tag{C.6}$$

C.2 Evaluation of Coefficients

Using the method outlined in the previous section, the values of the coefficients x and y can be calculated for different regions of approximation [22]. The coefficients for two, three, four and eight region approximations are listed in Tables C.1, C.2, C.3, and C.4 respectively. For more details see [22].

Table C.1 : Coefficients for Two Region Approximation

Region	x	y
$0 = b/a \leq 0.25$	0.9951	0.1234
$0.25 < b/a \leq 1.00$	0.8716	0.5176

Table C.2 : Coefficients for Three Region Approximation

Region	x	y
$0 = b/a \leq 0.25$	0.9951	0.1234
$0.25 < b/a \leq 0.625$	0.9225	0.3976
$0.625 < b/a \leq 1.00$	0.7813	0.6279

Table C.3 : Coefficients for four Region Approximation

Region	x	y
$0 = b/a \leq 0.25$	0.9951	0.1234
$0.25 < b/a \leq 0.50$	0.9392	0.3497
$0.50 < b/a \leq 0.75$	0.8506	0.5286
$0.75 < b/a \leq 1.00$	0.7547	0.6574

Table C.4 : Coefficients for Eight Region Approximation

Region	x	y
$0 = b/a \leq 0.125$	0.9987	0.0623
$0.125 < b/a \leq 0.25$	0.9835	0.1841
$0.25 < b/a \leq 0.375$	0.9952	0.2979
$0.375 < b/a \leq 0.50$	0.9168	0.4004
$0.50 < b/a \leq 0.625$	0.8722	0.4899
$0.625 < b/a \leq 0.75$	0.8246	0.5662
$0.75 < b/a \leq 0.875$	0.7767	0.6303
$0.875 < b/a \leq 1.00$	0.7300	0.6837

For the computation of the rms value, the peak value coefficients listed above can be divided by square root of 2. To implement the rms value computation these coefficients can be approximated by the nearest fraction powers of 2. The coefficients and their nearest approximations for computation of the rms values using four region approximation is listed below in Table C.5.

Table C.5 : Coefficients for RMS value computations.

Region	x	y
$0 = \frac{b}{a} \leq 0.25$	0.7036 (1 - 1/4 - 1/16 + 1/64 + 1/2048)	0.0873 (1/8 - 1/32 - 1/128 + 1/1024)
$0.25 < b/a \leq 0.50$	0.6641 (1/2 + 1/8 + 1/32 + 1/128)	0.2473 (1/4 - 1/512 - 1/1024)
$0.50 < b/a \leq 0.75$	0.6015 (1/2 + 1/8 - 1/32 + 1/128)	0.3738 (1/4 + 1/8 - 1/1024)
$0.75 < b/a \leq 1.00$	0.5336 (1/2 + 1/32 + 1/512 + 1/2048)	0.4648 (1/2 - 1/32 - 1/256)

APPENDIX - D

LOW PASS FILTER DESIGN

Designing filters based on the dedicated switched capacitor Low-Pass-Butterworth filters, MF4 and MF6, [27] is a fairly simple task since there are not many parameters that can be changed. Apart from selecting power supply voltages and clock logic levels, the only parameter that can be adjusted is the cutoff frequency. Therefore, the design task primarily involves deciding as to which device (MF4 or MF6) would be appropriate for a given application, selecting the necessary cutoff frequency, and calculating the required clock frequency.

The specifications of the filter to be designed are depicted in Figure D.1. The Gain of the filter should fall within the shaded area. This is a low-pass filter whose gain inside 80 Hz passband must not fall by more than 0.1 dB. At the stopband edge of 180 Hz, and at all higher frequencies, the gain must be at least 20 dB below the nominal passband gain of 0 dB. The order, n, of the filter can be determined by using Equation D.1.

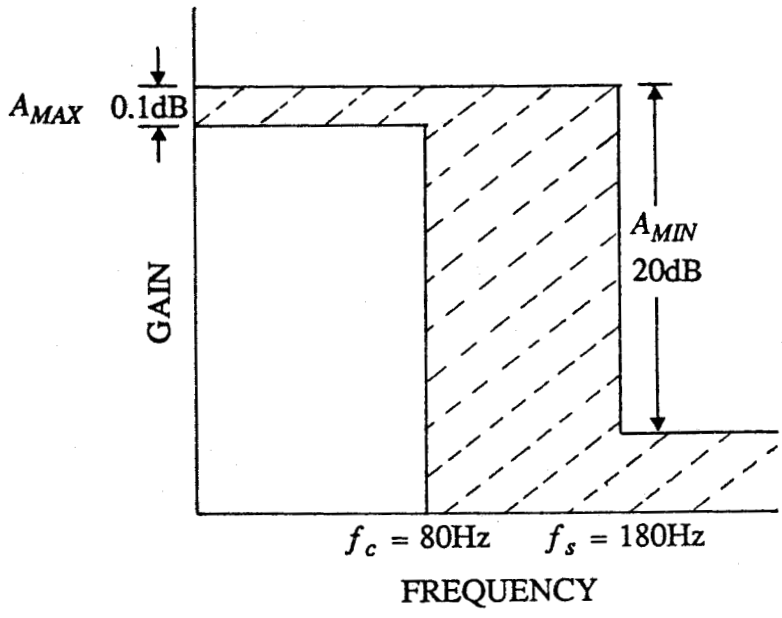

Figure D.1. Amplitude response requirements for the low pass filter.

$$n = \frac{\log_{10}\left[\frac{10^{A_{min}/10}-1}{10^{A_{max}/10}-1}\right]}{2\log_{10}\left[\frac{f_s}{f_c}\right]} \qquad \text{(D.1)}$$

where

f_c is frequency of the passband edge. However, f_c is *not* the same as the -3 dB frequency.

f_s is frequency of the stopband edge.

A_{max} is the maximum allowable gain variation in dB at frequencies below f_c. A_{max} is a positive number.

A_{min} is the minimum acceptable attenuation in dB at frequencies beyond f_s. A_{min} is a positive number.

For this example, $A_{min} = 20$, $A_{max} = 0.1$, $f_c = 80$ and $f_s = 180$. Inserting these values into Equation D.1 yields:

$$n = 5.15$$

Since n must be an integer, the next highest value which is 6, is taken. Therefore, an MF6 filter should be chosen for this application. Now that n has been determined, the attenuation in dB at f_s can be found from Equation D.2 given below:

$$A_{min} = 10\log_{10}\left[1+\left[10^{(0.1A_{max})}-1\right]\left[\frac{f_s}{f_c}\right]^{2n}\right] \qquad \text{(D.2)}$$

For $n = 6$ this value is found to be

$$A_{\min} = 25.9\ dB$$

Next, f_{-3dB} must be found. As stated before f_{-3dB}, which is the nominal cutoff frequency of the MF6, is different in this case from f_c. f_{-3dB} is needed in order to determine the clock frequency for the MF6. f_{-3dB} can be found from Equation D.3 given by:

$$\frac{f_{-3dB}}{f_c} = \left[\frac{10^{0.3} - 1}{10^{(0.1A_{max})} - 1}\right]^{1/2n} \qquad \text{(D.3)}$$

Substituting the values the nominal cutoff frequency is found to be

$$f_{-3dB} = 109.4Hz$$

The clock frequency will be $50 \times 109.4 = 5.47$ kHz for the MF6-50 and $100 \times 109.4 = 10.94$ kHz for the MF6-100. The MF6 can operate on a maximum clock frequency of 1 MHz. Circuit diagrams for various modes of operation of MF6 are shown in Figures D.2.

Alternatively, the MF6 filter can be used in self clock mode. This is useful in applications in which high accuracy of f_c is not needed. The external clock can be replaced by a resistor and a capacitor connected as shown in Figure D.2(c). The clock frequency obtained in the self clocking mode is given by Equation D.4.

$$f_{clk} = \frac{1}{1.69RC} \qquad \text{(D.4)}$$

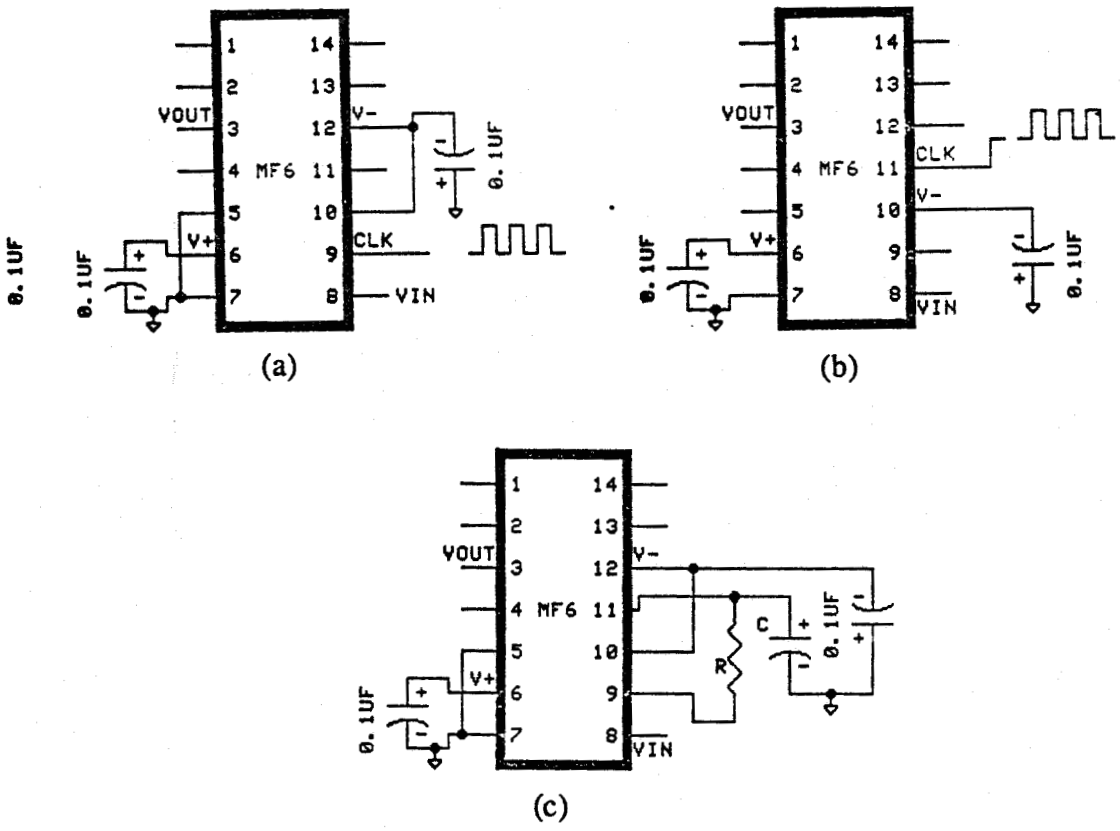

Figure D.2. Typical MF6 split supply application circuits. (a) CMOS clock levels. (b) TTL clock levels. (c) Self clocked operation using internal schmitt trigger.

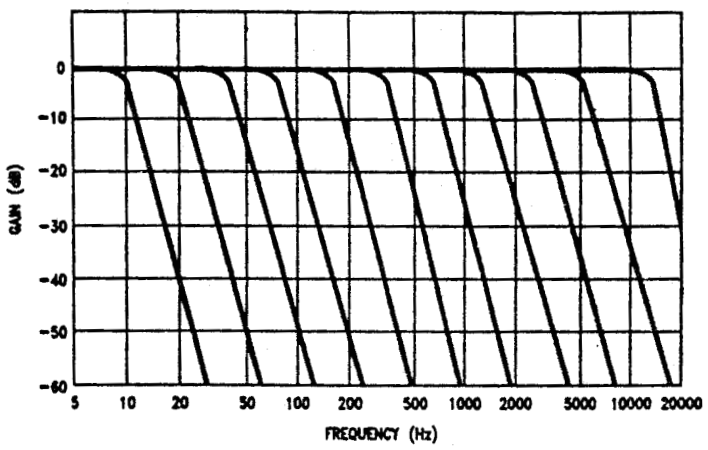

Figure D.3. Amplitude response of MF6 for several values of f_c .

The amplitude response of low pass sixth order Butterworth filter using MF6 is shown in figure D.3. The circuit diagram of the filter card designed for use in the project is shown in Figure D.4.

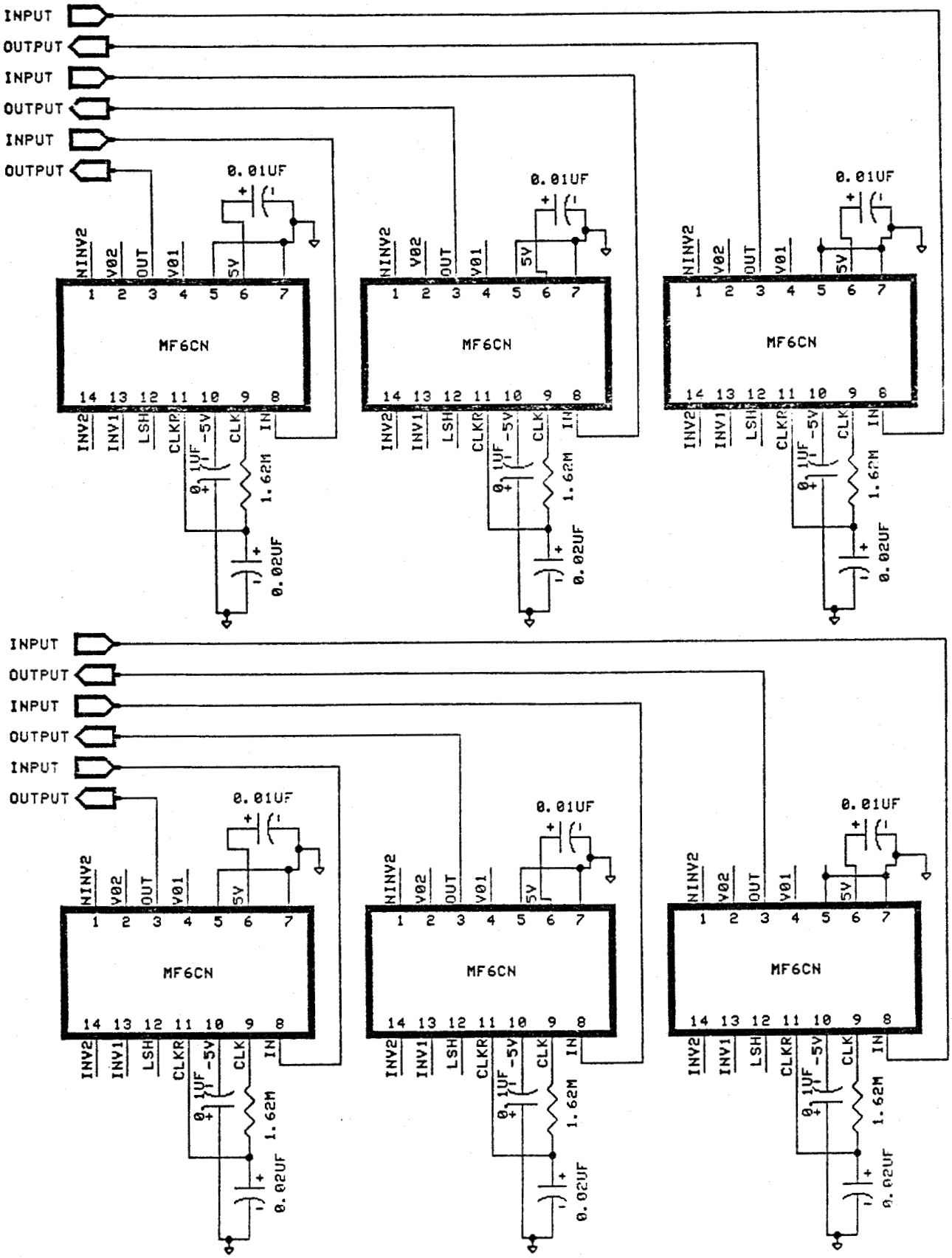

Figure D.4. Circuit diagram of the filter card designed for use in the project.

APPENDIX - E

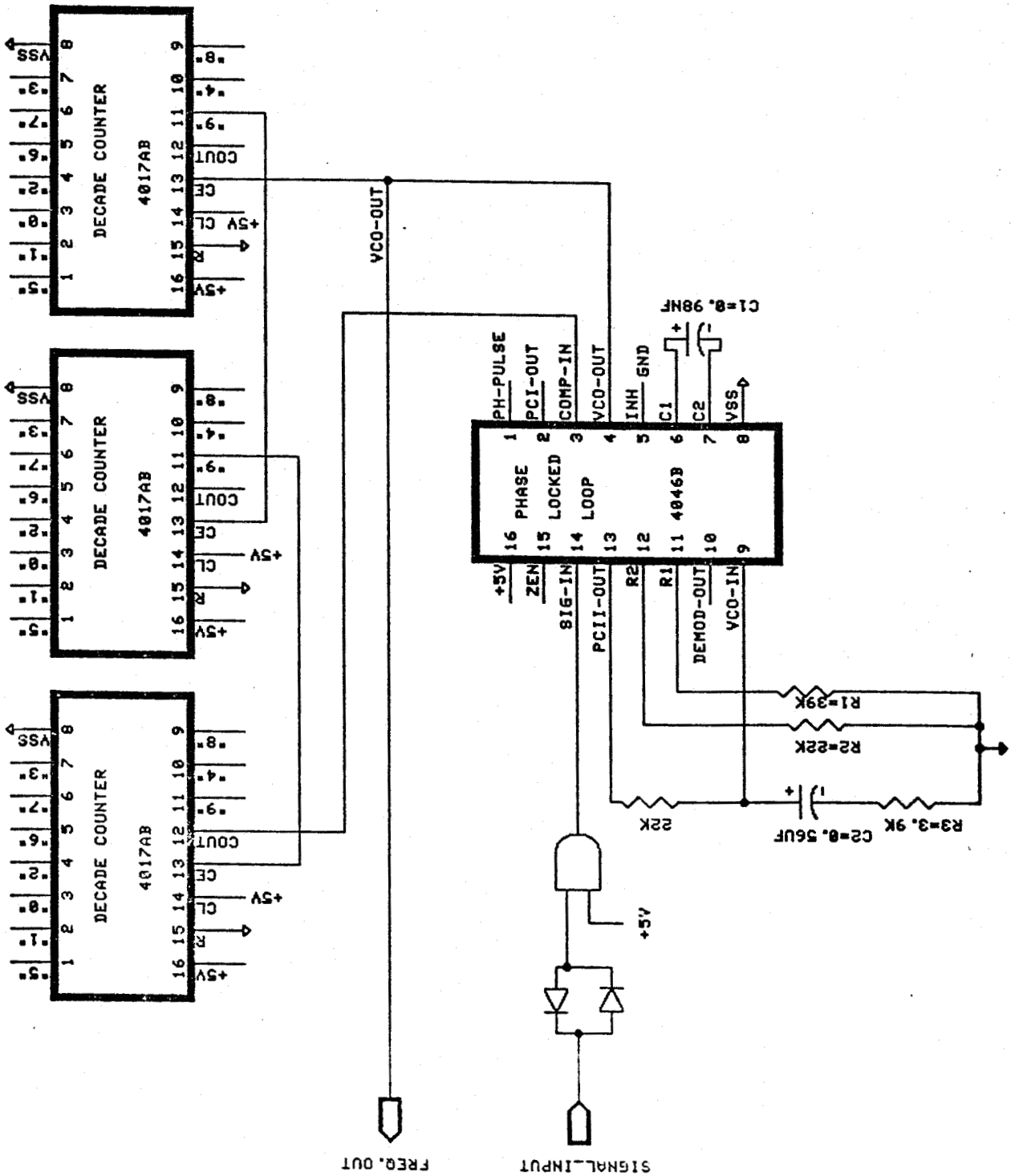

Figure E.1. Frequency Multiplier Unit Circuit Diagram.

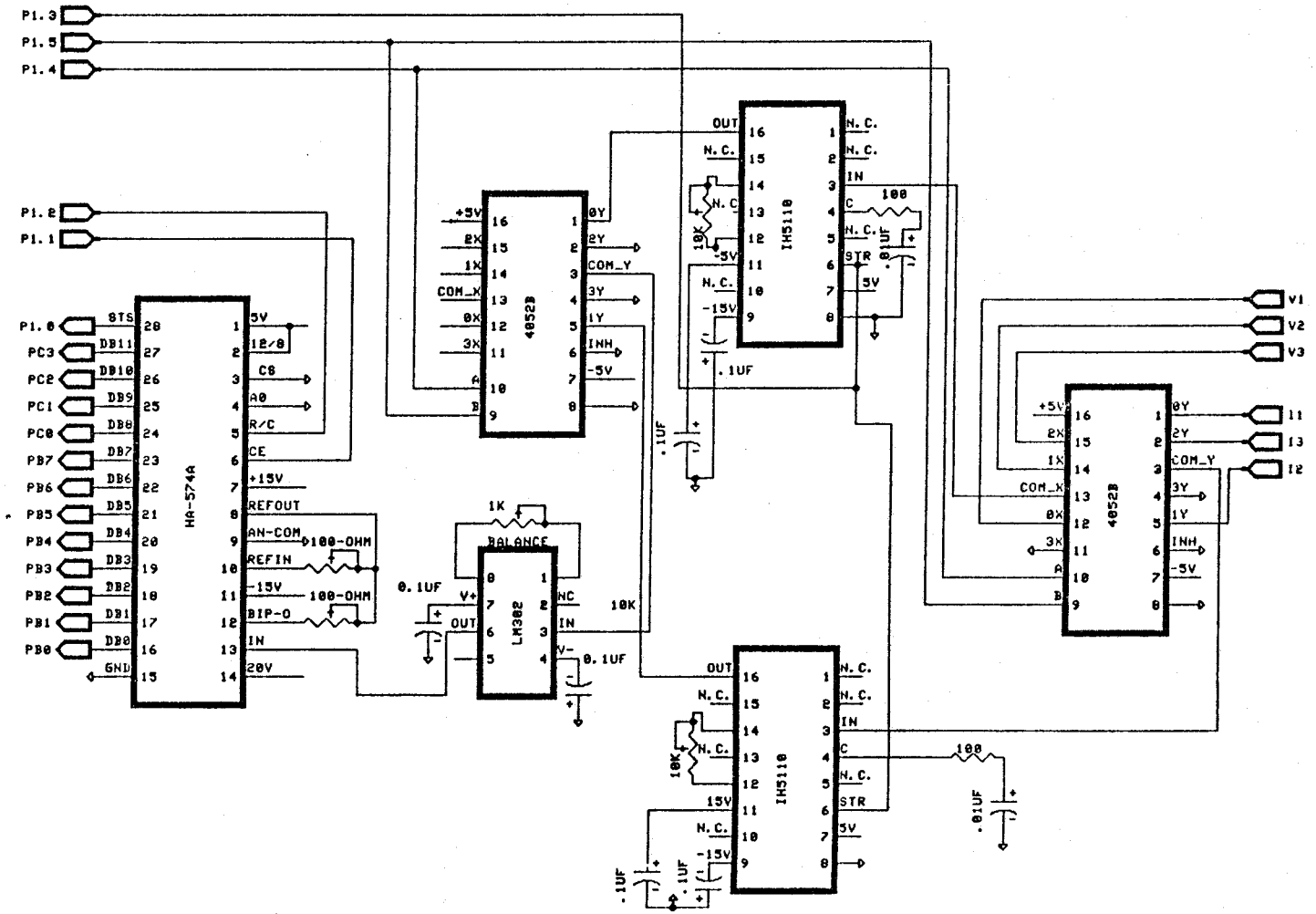

Figure F.1. Digitization Unit Circuit Diagram.

APPENDIX - G

PARAMETERS	PHASE-A	PHASE-B	PHASE-C
VOLTAGE (KV)	6.61	6.61	6.63
CURRENT (KA)	5.53	5.53	5.55
POWER FACTOR	0.92	0.92	0.91
ACTIVE POWER (KW)	33.52	33.52	33.52
REACTIVE POWER (KVA)	13.65	13.65	13.65
ENERGY (kWh)	0.85	0.85	0.85
ENERGY (kVArh)	0.30	0.30	0.30

FREQUENCY – 62.27 Hz